Pré-Publicações do Departamento de Matemática
Universidade de Coimbra
Preprint Number 08–28

SMART PLATES: REDUCED MODELS AND NUMERICAL SIMULATIONS

JOSÉ A. CARVALHO, ISABEL N. FIGUEIREDO AND REBECA MARTÍNEZ

Abstract: In this paper asymptotic models describing the mechanical and electric equilibrium state of two types of smart structures are presented and justified. The first structure consists of an anisotropic elastic thin plate with two surface bonded anisotropic piezoelectric patches and the second one is an anisotropic elastic sandwich thin plate with an inserted anisotropic piezoelectric patch. The two unknowns of the corresponding asymptotic models, the mechanical displacements of the structures and the electric potentials of the patches, are partially decoupled. The former are the solution of modified Kirchhoff-Love plate models, while the latter can be derived as explicit functions of the mechanical displacements. Moreover, different formulas for the electric potential arise as a consequence of diverse electric boundary conditions. We report numerical simulations with these asymptotic models.

Keywords: piezoelectricity, anisotropic material, elasticity, plate.

1. Introduction

Smart structures are advanced structures that consist generally of a host structure (for instance a plate, a beam or a shell) with integrated surface-bonded or embedded devices of active or smart materials (cf. [26]). These devices have the capability to change the structure's behavior acting as sensors and actuators, with the purpose of obtaining a self-controlled and self-adaptive structure able to react and adapt to the environment. The sensors give information about the state of the structure, while the actuators can generate modifications in its mechanical behavior. The most used smart materials are piezoelectric materials, which have the property to convert mechanical energy into electric energy and vice-versa. Therefore piezoelectric devices are both actuators and sensors. This makes them useful in a wide range of practical applications, where their geometries are those of thin plates (i.e. the thickness is very small when compared to the area of the middle plane of the plate).

The aim of this paper is to describe and mathematically justify asymptotic models for static thin plate structures made of elastic plates with integrated piezoelectric patches or layers. In short, these asymptotic models are reduced

Received June 11, 2008.

(i.e. lower-dimensional) models resulting from the application of a mathematical procedure (termed the asymptotic method) that aims to compute the behavior of the solutions of the three-dimensional equilibrium variational equations, as the thicknesses (of the structures) approach zero.

We refer to [5, 6, 8] and [7] for an overview of the application of the asymptotic method to elastic plates and junctions in elastic multi-structures, respectively, and to [9] and [29] for elastic shells and rods, respectively. In the literature there are also articles reporting reduced models obtained with the asymptotic method, for plates, shells or rods made exclusively of piezoelectric materials (cf. [20, 21, 22, 23, 24, 25, 30, 10, 15, 16, 17]). In all these articles the asymptotic modelling of an assemblage of elastic and piezoelectric constituents is not analyzed. However that in [4] reduced models are proposed for thin smart shells with piezoelectric patches; but those are derived without applying the asymptotic variational method, but rather using convenient a priori mechanical and electric assumptions. There are also articles concerning the mathematical analysis (see [13, 27, 28]), numerical analysis and numerical simulations (see [18, 14, 1, 2, 3]) for two and three-dimensional models involving exclusively piezoelectric materials, and not a mixture of different elastic and piezoelectric materials.

In this paper two types of smart structures are considered : one (termed PSBP) concerns an elastic thin plate with two surface bonded piezoelectric patches and the other one (termed PIP) an elastic sandwich thin plate with an inserted piezoelectric patch. In the corresponding asymptotic models, it is found that the solution is the pair composed by the mechanical displacement of the structure, which is a Kirchhoff-Love displacement, and the electric potential of the patches, which is a function of the mechanical displacement. These asymptotic models are two-dimensional models, defined on the middle plane of the structures. In addition, in the three-dimensional models, it is assumed that each piezoelectric patch verifies a mixed Dirichlet-Neumann electric boundary condition and it is supposed that there are three possible parts of the patch's boundary where the Dirichlet conditon can act (a part of the patch's lateral boundary together with both the upper and lower faces of the patch, or together with just the upper or the lower surface of the patch). Actually these three possibilities give rise to three distinct formulas for the patch's electric potential.

It is significant to say that the asymptotic models of this paper are in good agreement with those proposed in [4] for thin smart shells with piezoelectric

patches (a plate is also a shell with a plane middle surface). More specifically, as in [4], we also found out that the asymptotic electric potentials are quadratic polynomials with respect to the thickness variable.

We emphasize that all the materials (both elastic and piezoelectric) under consideration are mechanically and electrically anisotropic, but not completely non homogeneous, since it is assumed that all the material coefficients are independent of the thickness variable. But an important point is that this assumption is by no means restrictive, it is only used for the sake of simplicity of the formulas involved in the definition of the asymptotic models (cf. (1)–(3)). In addition, it is significant to mention that this simplification does not lead to easier asymptotic models. Actually it is found that the tangential and transverse components of the mechanical displacement are coupled, unless the different constituent materials are equal and symmetrically disposed with respect to the middle plane of the global structure (cf. corollaries 3.1 and 3.2 for PSBP and corollaries 4.1 and 4.2 for PIP).

Furthermore, it is worthwhile to remark that the asymptotic models presented here easily generalize to the case of structures that have a finite number of surface bonded or inserted piezoelectric patches. Moreover different asymptotic models can be obtained depending on the possible combinations of the electric boundary conditions (among the three types mentioned above) for the different patches integrated in the structure. From the physical point of view, this means that some of the patches may act like actuators, while the remaining other ones may behave like sensors. In this way the structure becomes a smart or an active one.

The mathematical justification of the two asymptotic models (for PSBP and PIP) presented in this paper, strongly relies on the arguments reported on the papers [12, 15, 17, 25], for the piezoelectric patches (which have the geometry of plates) and [8] for the elastic plates. In reality the mathematical reasoning, that leads to the asymptotic models for PSBP and PIP, is a judicious combination of the proofs presented in these above mentioned works. In short, it is enough to take into account the specific geometry of the global structure, to assume the integrated piezoelectric patches are perfectly surface-bonded or embedded (so that in the three-dimensional equilibrium equations, the mechanical displacements and the stresses are continuous at the interfaces of the materials (cf. (11) and (28)) and to combine carefully the three different possible choices of electric boundary conditions for the

piezoelectric patches. Consequently, the proofs for the asymptotic models for PSBP and PIP are only briefly sketched and not detailed in this paper.

After this introduction the remainder of the paper consists of four sections. Section 2 describes the notation as well as a short summary of the asymptotic method. In sections 3 and 4 the asymptotic models are defined. The organization of these sections 3 and 4 is very similar. Firstly the three-dimensional mechanical and electric equilibrium equations are defined. On the whole these consist of several groups of equilibrium equations modelling each part of the structure (either elastic or piezoelectric) together with the boundary conditions and the transmission conditions at the interfaces of the different constituents. Next, the asymptotic models are stated in theorems 3.1, 3.2 and 3.3 for the PSBP structure and theorems 4.1, 4.2 and 4.3 for the PIP structure. Corollaries of these theorems, which arise for particular symmetric geometries, materials and data of the patches, are also stated and demonstrated. Finally in section 5 we present the numerical tests.

2. Notations and asymptotic method

2.1. Geometry. Let (O, x_1, x_2, x_3) be a cartesian three-dimensional reference system and $\omega \subset \mathbb{R}^2$ be a bounded domain with a Lipschitz continuous boundary, and ω^{mat} a subset of ω. For each $0 < h \leq 1$ we consider the set $\Omega = \omega \times (-h, h)$. An arbitrary point of Ω is denoted by $x = (x_1, x_2, x_3)$, where the first two components $(x_1, x_2) = (x_1, x_2) \in \omega$ are independent of h and $x_3 \in (-h, h)$.

In the sequel, in sections 3 and 4, we consider that the plate Ω is made of one or two elastic materials with integrated piezoelectric patches. This means that $\Omega = \omega \times (-h, h) = \cup_{mat} \Omega^{mat}$ where the abbreviation mat stands for material and each subset $\Omega^{mat} = \omega^{mat} \times (z^{mat} - \frac{t^{mat}}{2}, z^{mat} + \frac{t^{mat}}{2})$ represents either the elastic plate or the piezoelectric patches, which are also plates. The positive scalar t^{mat} represents the thickness of the plate Ω^{mat}. The absolute value $|z^{mat}|$ is the distance, measured along the thickness axis, from the middle plane of Ω^{mat} to the x_1x_2-plane of the global reference system (O, x_1, x_2, x_3).

Moreover let $\partial\Omega$ be the boundary of Ω and $\gamma_0 \subset \partial\omega$ a subset of the boundary $\partial\omega$ of ω, such that, $meas(\gamma_0) \neq 0$ and $\gamma_1 = \partial\omega \setminus \gamma_0$. In addition, we define $\gamma_e^{mat} \subset \partial\omega^{mat}$ which is a subset of the boundary $\partial\omega^{mat}$ of ω^{mat} and $\gamma_s^{mat} = \partial\omega^{mat} \setminus \gamma_e^{mat}$. We denote by $\nu = (\nu_1, \nu_2, \nu_3)$ the outward unit normal

vector to the boundary $\partial\Omega$, where $\nu = (\nu_1, \nu_2) = (\nu_\alpha)$ is the unit outer normal vector along $\partial\omega$.

Given a function $\theta(x)$ defined in Ω we denote by $\partial_i\theta$ its partial derivative with respect to x_i, that is, $\partial_i\theta = \frac{\partial\theta}{\partial x_i}$ and by $\partial_{\alpha\beta}\theta = \frac{\partial^2\theta}{\partial x_\alpha \partial x_\beta}$ is the second partial derivative of θ with respect to x_α and x_β.

2.2. Materials. Throughout the paper, the latin indices i, j, k, l... belong to the set $\{1,2,3\}$, the greek indices α, β, μ... vary in the set $\{1,2\}$ and the summation convention with respect to repeated indices is employed, that is, $a_i b_i = \sum_{i=1}^3 a_i b_i$. Moreover we denote by $a \cdot b = a_i b_i$ the inner product of the vectors $a = (a_i)$ and $b = (b_i)$, by $Ce = (C_{ijkl} e_{kl})$ the contraction of a fourth order tensor $C = (C_{ijkl})$ with a second order tensor $e = (e_{kl})$ and by $Ce : d = C_{ijkl} e_{kl} d_{ij}$ the inner product of the tensors Ce and $d = (d_{ij})$.

We also denote by $C^{mat} = (C^{mat}_{ijkl})$, $P^{mat} = (P^{mat}_{ijkl})$ and $\varepsilon^{mat} = (\varepsilon^{mat}_{ij})$ the fourth, third and second order tensors, respectively, representing the elastic, piezoelectric and dielectric coefficients of a plate made of a material denoted by *mat* and occupying the three-dimensional plate Ω^{mat}. For an elastic material *mat* only the tensor C^{mat} is defined but if *mat* is a piezoelectric material the three tensors C^{mat}, P^{mat} and ε^{mat} are required.

We introduce now the modified coefficients $A^{mat}_{\alpha\beta\gamma\rho}$, $p^{mat}_{3\alpha\beta}$ and p^{mat}_{33} depending only on C^{mat}_{ijkl}, P^{mat}_{ijk} and ε^{mat}_{ij} and that are defined by (cf. formula (8) in [12])

$$A^{mat}_{\alpha\beta\gamma\rho} = C^{mat}_{\alpha\beta\gamma\rho} - \frac{C^{mat}_{\alpha\beta 33} C^{mat}_{33\gamma\rho}}{C^{mat}_{3333}} + \left(C^{mat}_{\alpha\beta 33} \frac{C^{mat}_{\nu 333}}{C^{mat}_{3333}} - C^{mat}_{\alpha\beta\nu 3} \right) b^{mat}_{\delta\nu}\, a^{mat}_{\delta\gamma\rho},$$

$$p^{mat}_{3\alpha\beta} = P^{mat}_{3\alpha\beta} - \frac{C^{mat}_{\alpha\beta 33}}{C^{mat}_{3333}} P^{mat}_{333} + \left(C^{mat}_{\alpha\beta 33} \frac{C^{mat}_{33\nu 3}}{C^{mat}_{3333}} - C^{mat}_{\alpha\beta\nu 3} \right) b^{mat}_{\delta\nu}\, c^{mat}_{\delta},$$

$$p^{mat}_{33} = \varepsilon^{mat}_{33} + \frac{P^{mat}_{333} P^{mat}_{333}}{C^{mat}_{3333}} - \left(P^{mat}_{333} \frac{C^{mat}_{33\nu 3}}{C^{mat}_{3333}} - P^{mat}_{3\nu 3} \right) b^{mat}_{\delta\nu}\, c_\delta,$$

where

$$a^{mat}_{\delta\gamma\rho} = C^{mat}_{33\gamma\rho} C^{mat}_{\delta 333} - C^{mat}_{\delta 3\gamma\rho} C^{mat}_{3333}, \qquad c^{mat}_{\delta} = C^{mat}_{\delta 333} P^{mat}_{333} - C^{mat}_{3333} P^{mat}_{3\delta 3},$$

$$[b^{mat}_{\delta\nu}] = [C^{mat}_{\delta 333} C^{mat}_{33\nu 3} - C^{mat}_{\delta 3\nu 3} C^{mat}_{3333}]^{-1} \quad \text{(identity between two matrices)}.$$

We always assume that the material *mat*, either elastic or piezoelectric, is such that the corresponding material coefficients are independent of the thickness variable x_3 (actually, commonly used piezoelectric materials are

transverse isotropic like PZT (lead-zirconate titanate), or orthorhombic like PVDF (polyvinylidene fluoride)).

In the following sections we use several matrices which are associated to these modified coefficients. For each material mat, these matrices have their components multiplied by the characteristic function $\chi_{\omega^{mat}}$ (if $x \in \omega^{mat}$ then $\chi_{\omega^{mat}}(x) = 1$, and if $x \notin \omega^{mat}$ then $\chi_{\omega^{mat}}(x) = 0$). The matrices are denoted by A_i^{mat} for $i = 0, 1, 2$, p_j^{mat} for $j = 1, 2$ and pp_k^{mat} for $k = 0, 1, 2$. The components of A_i^{mat} are defined by

$$
\begin{aligned}
(A_0^{mat})_{\alpha\beta\gamma\rho} &= \chi_{\omega^{mat}} \int_{z^{mat}-\frac{t^{mat}}{2}}^{z^{mat}+\frac{t^{mat}}{2}} A^{mat}_{\alpha\beta\gamma\rho}\, dx_3 = \chi_{\omega^{mat}} A^{mat}_{\alpha\beta\gamma\rho}\, t^{mat} \\
(A_1^{mat})_{\alpha\beta\gamma\rho} &= \chi_{\omega^{mat}} \int_{z^{mat}-\frac{t^{mat}}{2}}^{z^{mat}+\frac{t^{mat}}{2}} x_3\, A^{mat}_{\alpha\beta\gamma\rho}\, dx_3 = \chi_{\omega^{mat}} A^{mat}_{\alpha\beta\gamma\rho}\, t^{mat}\, z^{mat} \\
(A_2^{mat})_{\alpha\beta\gamma\rho} &= \chi_{\omega^{mat}} \int_{z^{mat}-\frac{t^{mat}}{2}}^{z^{mat}+\frac{t^{mat}}{2}} x_3^2\, A^{mat}_{\alpha\beta\gamma\rho}\, dx_3 = \chi_{\omega^{mat}} A^{mat}_{\alpha\beta\gamma\rho}\, \tfrac{1}{12}\big((t^{mat})^3 + 12\, t^{mat}\, (z^{mat})^2\big).
\end{aligned}
\tag{1}
$$

The components of p_j^{mat} for $j = 1, 2$ are given by

$$
\begin{aligned}
(p_1^{mat})_{\alpha\beta\gamma\rho} &= \chi_{\omega^{mat}} \int_{z^{mat}-\frac{t^{mat}}{2}}^{z^{mat}+\frac{t^{mat}}{2}} \frac{p^{mat}_{3\alpha\beta}\, p^{mat}_{3\gamma\rho}}{p^{mat}_{33}}\, (x_3 - z^{mat})\, dx_3 = 0 \\
(p_2^{mat})_{\alpha\beta\gamma\rho} &= \chi_{\omega^{mat}} \int_{z^{mat}-\frac{t^{mat}}{2}}^{z^{mat}+\frac{t^{mat}}{2}} \frac{p^{mat}_{3\alpha\beta}\, p^{mat}_{3\gamma\rho}}{p^{mat}_{33}}\, (x_3 - z^{mat})\, x_3\, dx_3 = \chi_{\omega^{mat}} \frac{p^{mat}_{3\alpha\beta}\, p^{mat}_{3\gamma\rho}}{p^{mat}_{33}}\, \frac{(t^{mat})^3}{12},
\end{aligned}
\tag{2}
$$

Finally the components of pp_k^{mat} for $k = 0, 1, 2$ are defined

$$
\begin{aligned}
(pp_0^{mat})_{\alpha\beta\gamma\rho} &= \chi_{\omega^{mat}} \int_{z^{mat}-\frac{t^{mat}}{2}}^{z^{mat}+\frac{t^{mat}}{2}} \frac{p^{mat}_{3\alpha\beta}\, p^{mat}_{3\gamma\rho}}{p^{mat}_{33}}\, dx_3 = \chi_{\omega^{mat}} \frac{p^{mat}_{3\alpha\beta}\, p^{mat}_{3\gamma\rho}}{p^{mat}_{33}}\, t^{mat} \\
(pp_1^{mat})_{\alpha\beta\gamma\rho} &= \chi_{\omega^{mat}} \int_{z^{mat}-\frac{t^{mat}}{2}}^{z^{mat}+\frac{t^{mat}}{2}} \frac{p^{mat}_{3\alpha\beta}\, p^{mat}_{3\gamma\rho}}{p^{mat}_{33}}\, x_3\, dx_3 = \chi_{\omega^{mat}} \frac{p^{mat}_{3\alpha\beta}\, p^{mat}_{3\gamma\rho}}{p^{mat}_{33}}\, t^{mat}\, z^{mat} \\
(pp_2^{mat})_{\alpha\beta\gamma\rho} &= \chi_{\omega^{mat}} \int_{z^{mat}-\frac{t^{mat}}{2}}^{z^{mat}+\frac{t^{mat}}{2}} \frac{p^{mat}_{3\alpha\beta}\, p^{mat}_{3\gamma\rho}}{p^{mat}_{33}} x_3^2 dx_3 = \chi_{\omega^{mat}} \frac{p^{mat}_{3\alpha\beta} p^{mat}_{3\gamma\rho}}{p^{mat}_{33}} \frac{1}{12}\big((t^{mat})^3 + 12\, t^{mat}\, (z^{mat})^2\big).
\end{aligned}
\tag{3}
$$

2.3. Functional spaces. Now let Ξ represent any open subset of $\mathbb{R}^n$, with $n = 2, 3$. We use the Sobolev spaces $H^m(\Xi)$ (also denoted by $W^{m,2}(\Xi)$), defined by

$$
\begin{aligned}
H^1(\Xi) &= \big\{v \in L^2(\Xi) : \quad \partial_i v \in L^2(\Xi), \quad \text{for } i = 1, \ldots, n\big\}, \\
H^2(\Xi) &= \big\{v \in L^2(\Xi) : \quad \partial_i v,\ \ \partial_{ij} v \in L^2(\Xi), \quad \text{for } i, j = 1, \ldots, n\big\},
\end{aligned}
$$

where $L^2(\Xi) = \{v : \Xi \to \mathbb{R}, \quad \int_\Xi |v|^2 d\Xi < +\infty\}$ and the partial derivatives are interpreted as distributional derivatives.

We use as well the space V_{KL}, associated to the admissible mechanical displacements, and the spaces Ψ_l^{mat} and Ψ_{l0}^{mat}, associated to the electric potentials, defined by

$$\begin{aligned} V_{KL} &= \{v \in [H^1(\Omega)]^3 : \quad v_{|\Gamma_D} = 0, \quad e_{i3}(v) = 0\}, \\ \Psi_l^{mat} &= \{\psi^{mat} \in L^2(\Omega^{mat}) : \quad \partial_3 \psi^{mat} \in L^2(\Omega^{mat})\}, \\ \Psi_{l0}^{mat} &= \{\psi^{mat} \in L^2(\Omega^{mat}) : \quad \partial_3 \psi^{mat} \in L^2(\Omega^{mat}), \quad \psi^{mat}_{|\Gamma_{eD}^{mat}} = 0\}, \end{aligned} \tag{4}$$

where $e_{i3}(v) = \frac{1}{2}(\partial_i v_3 + \partial_3 v_i)$ and Γ_D, Γ_{eD}^{mat} are subsets of the boundary $\partial\Omega$ of Ω (cf. (6), (7) for PSBP and (23), (24) for PIP). The space V_{KL}, which is the so-called Kirchhoff-Love mechanical displacement space, is equivalently defined by (cf. [8], p. 47)

$$\begin{aligned} V_{KL} = \Big\{ & v = (v_1, v_2, v_3) \in [H^1(\Omega)]^3 : \quad \exists \eta = (\eta_1, \eta_2, \eta_3) \in [H^1(\omega)]^2 \times H^2(\omega), \\ & v_\alpha(x) = \eta_\alpha(x_1, x_2) - x_3\, \partial_\alpha \eta_3(x_1, x_2), \quad v_3(x) = \eta_3(x_1, x_2), \\ & \eta_{1_{|\gamma_0}} = \eta_{2_{|\gamma_0}} = \eta_{3_{|\gamma_0}} = 0, \quad \partial_\nu \eta_{3_{|\gamma_0}} = 0 \Big\}. \end{aligned}$$

2.4. Asymptotic method. The asymptotic method can be briefly described as follows. Starting with the three-dimensional equilibrium variational equations for a plate with global thickness h, these equations are scaled to a domain that is independent of h. Assuming appropriate scalings for the data and unknowns, one then lets $h \to 0$ and studies the convergence of the unknowns in appropriate functional spaces. This leads to the definition of the limit model and rescaling it to the original domain then results the asymptotic model (also termed reduced or lower-dimensional model).

3. Plate with surface bonded patches – PSBP

Here we define the reduced model for a PSBP structure. It is obtained by applying the asymptotic method to the three-dimensional equilibrium variational equations of a PSBP structure, and its definition is stated in theorem 3.1. Particular formulations of this reduced model are described in theorems 3.2 and 3.3, for different electric boundary conditions on the piezoelectric patches.

3.1. The three-dimensional model – PSBP. We consider a thin elastic plate with two piezoelectric patches bonded on its lower and upper surfaces, respectively. In the following the geometrical and material properties of the two patches and the elastic plate are indexed by the upper subscripts $-$ or $+$ for the lower or upper patch respectively, and m for the elastic plate (meaning in the middle or between the two patches).

The geometry of this structure is then defined by the three-dimensional set $\Omega = \cup_{mat}\Omega^{mat} = \Omega^- \cup \Omega^m \cup \Omega^+$, which has global thickness $2h$ (where $h > 0$ is a small parameter) and such that

$$\begin{aligned} \Omega^- &= \omega^- \times (z^- - \tfrac{t^-}{2}, z^- + \tfrac{t^-}{2}), \\ \Omega^m &= \omega \times (z^m - \tfrac{t^m}{2}, z^m + \tfrac{t^m}{2}), \\ \Omega^+ &= \omega^+ \times (z^+ - \tfrac{t^+}{2}, z^+ + \tfrac{t^+}{2}). \end{aligned} \tag{5}$$

The two sets Ω^- and Ω^+ define the geometry of the two patches and Ω^m the geometry of the elastic plate. The positive scalars t^-, t^m and t^+ represent the thicknesses of layers Ω^-, Ω^m and Ω^+, respectively, and verify $t^- + t^m + t^+ = 2h$. The absolute values $|z^-|$, $|z^m|$ and $|z^+|$ are the distances, measured along the thickness axis, from the middle plane of Ω to the middle plane of layers Ω^-, Ω^m and Ω^+, respective

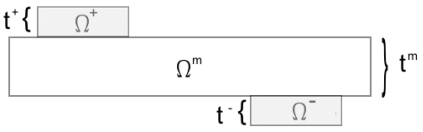

FIGURE 1. Vertical cross section along the thickness for a rectangular plate with two piezoelectric patches

We remark that ω^- and ω^+ are subsets of ω. Moreover, we define the boundary sets

$$\begin{aligned} &\Gamma_D^m = \gamma_0 \times (z^m - \tfrac{t^m}{2}, z^m + \tfrac{t^m}{2}), \qquad \Gamma_N^m = \Gamma \setminus \Gamma_D^m, \\ &\Gamma_{up/lo}^{mat} = \Gamma_{lo}^{mat} \cup \Gamma_{up}^{mat}, \quad \Gamma_{lo}^{mat} = \omega^{mat} \times \{z^{mat} - \tfrac{t^{mat}}{2}\}, \\ &\Gamma_{up}^{mat} = \omega^{mat} \times \{z^{mat} + \tfrac{t^{mat}}{2}\}, \\ &\Gamma_s^{mat} = \gamma_s^{mat} \times (z^{mat} - \tfrac{t^{mat}}{2}, z^{mat} + \tfrac{t^{mat}}{2}), \\ &\Gamma_e^{mat} = \gamma_e^{mat} \times (z^{mat} - \tfrac{t^{mat}}{2}, z^{mat} + \tfrac{t^{mat}}{2}), \end{aligned} \tag{6}$$

for $mat = +, -$. In addition, we also introduce three different disjoint partitions $\{\Gamma_{eD}^{mat}, \Gamma_{eN}^{mat}\}$ of the boundary of Ω^{mat}, for $mat = +, -$, defined by

$$\begin{aligned}
&(ebc1^{mat}): \qquad \Gamma_{eN}^{mat} = \Gamma_{s}^{mat}, \qquad \text{and} \quad \Gamma_{eD}^{mat} = \Gamma_{up/lo}^{mat} \cup \Gamma_{e}^{mat},\\
&(ebc2^{mat}): \qquad \Gamma_{eN}^{mat} = \Gamma_{s}^{mat} \cup \Gamma_{up}^{mat} \quad \text{and} \quad \Gamma_{eD}^{mat} = \Gamma_{lo}^{mat} \cup \Gamma_{e}^{mat},\\
&(ebc3^{mat}): \qquad \Gamma_{eN}^{mat} = \Gamma_{s}^{mat} \cup \Gamma_{lo}^{mat} \quad \text{and} \quad \Gamma_{eD}^{mat} = \Gamma_{up}^{mat} \cup \Gamma_{e}^{mat}.
\end{aligned} \tag{7}$$

The three-dimensional model, representing the mechanical and electric equilibrium state of the PSBP structure with geometry Ω, aims to find the mechanical displacement u defined in $\Omega = \Omega^- \cup \Omega^m \cup \Omega^+$ and the electric potentials φ^- and φ^+, defined in Ω^- and Ω^+, respectively, satisfying the following system of equations and boundary conditions:

$$\left[\begin{array}{ll} -\operatorname{div}\sigma = f & \text{in} \quad \Omega^- \cup \Omega^m \cup \Omega^+\\ \operatorname{div} D = r & \text{in} \quad \Omega^- \cup \Omega^+, \end{array}\right. \tag{8}$$

$$u = 0 \quad \text{on} \quad \Gamma_D^m \quad \text{and} \quad \sigma \cdot \nu = g \quad \text{on} \quad \Gamma_N^m, \tag{9}$$

$$\left[\begin{array}{lll} D\cdot\nu = \theta & \text{on} & \Gamma_{eN}^-\\ \varphi^- = \varphi_0^- & \text{on} & \Gamma_{eD}^- \end{array}\right. \quad \text{and} \quad \left[\begin{array}{lll} D\cdot\nu = \theta & \text{on} & \Gamma_{eN}^+\\ \varphi^+ = \varphi_0^+ & \text{on} & \Gamma_{eD}^+, \end{array}\right. \tag{10}$$

$$\left[\begin{array}{llll} u^m = u^- & \text{and} & (\sigma^m - \sigma^-)\cdot\nu = 0 & \text{on} \quad \Omega^- \cap \Omega^m = \omega^- \times \{z^m - \frac{t^m}{2}\}\\ u^m = u^+ & \text{and} & (\sigma^m - \sigma^+)\cdot\nu = 0 & \text{on} \quad \Omega^+ \cap \Omega^m = \omega^+ \times \{z^m + \frac{t^m}{2}\}, \end{array}\right. \tag{11}$$

$$\left[\begin{array}{lll} \text{in} \quad \Omega^m: & \sigma = C^m \cdot e(u) & \\ \text{in} \quad \Omega^-: & \left[\begin{array}{l} \sigma = C^- \cdot e(u) - P^- \cdot E(\varphi^-)\\ D = P^- \cdot e(u) + \varepsilon^- \cdot E(\varphi^-) \end{array}\right. & \\ \text{in} \quad \Omega^+: & \left[\begin{array}{l} \sigma = C^+ \cdot e(u) - P^+ \cdot E(\varphi^+)\\ D = P^+ \cdot e(u) + \varepsilon^+ \cdot E(\varphi^+). \end{array}\right. & \end{array}\right. \tag{12}$$

The equations (8) are the mechanical equilibrium equations and Maxwell-Gauss equations: σ is the stress tensor field, D is the electric displacement vector field, f and r are the densities of applied body forces and volume electric charge, respectively, acting on the plate Ω. The mechanical boundary conditions are defined in (9), meaning that the plate is clamped on Γ_D^m and submitted to the density of applied surface forces g on Γ_N^m. The electrical boundary conditions are defined in (10) and mean that the plate is submitted

to applied electric potentials, φ_0^- and φ_0^+ on Γ_{eD}^- and Γ_{eD}^+ respectively, and to a surface electric charge of density θ on Γ_{eN}^- and Γ_{eN}^+. The equations (11) represent the transmission conditions at the interfaces and finally (12) are the constitutive equations that evidence the converse (actuator) and direct (sensor) effects of the patches. In (12) the tensors C^m, C^- and C^+ represent the elasticity coefficients of the elastic, lower and upper piezoelectric patches, and finally P^-, P^+ and ε^-, ε^+ are the piezoelectric and dielectric tensors of the lower and upper piezoelectric patches. Moreover the notation σ^m, σ^+ and σ^- in (11) is self-evident and stands for the restriction of σ to Ω^m, Ω^+ and Ω^- respectively.

3.2. The asymptotic model – PSBP.

Theorem 3.1. *Let us assume any type of electric boundary conditions* $(ebci^{mat})$ *with* $i = 1, 2, 3$ *and* $mat = +, -$. *Then, the (variational) asymptotic model corresponding to problem* (8)-(12) *is*

$$\begin{cases} \text{Find} \quad (u, \varphi^+, \varphi^-) \in V_{KL} \times \Psi_l^+ \times \Psi_l^- \quad \text{such that:} \\ a\Big((u, \varphi^+, \varphi^-), (v, \psi^+, \psi^-)\Big) = l(v, \psi^+, \psi^-), \quad \forall (v, \psi^+, \psi^-) \in V_{KL} \times \Psi_{l0}^+ \times \Psi_{l0}^-, \\ \varphi^{mat} = \varphi_0^{mat}, \quad \text{on} \quad \Gamma_{eD}^{mat}, \quad \text{for } mat = +, -, \end{cases} \tag{13}$$

where

$$a\Big((u, \varphi^+, \varphi^-), (v, \psi^+, \psi^-)\Big) = a^m(u, v) + a^+\Big((u, \varphi^+), (v, \psi^+)\Big) + a^-\Big((u, \varphi^-), (v, \psi^-)\Big),$$

$$a^m(u, v) = \int_{\Omega^m} A^m_{\alpha\beta\gamma\rho} e_{\alpha\beta}(u)\, e_{\gamma\rho}(v)\, dx,$$

$$\begin{aligned} a^{mat}\Big((u, \varphi^{mat}), (v, \psi)\Big) \;=\; & \int_{\Omega^{mat}} A^{mat}_{\alpha\beta\gamma\rho} e_{\alpha\beta}(u)\, e_{\gamma\rho}(v)\, dx + \int_{\Omega^{mat}} p^{mat}_{33}\, \partial_3\varphi^{mat}\, \partial_3\psi^{mat}\, dx \\ & - \int_{\Omega^{mat}} p^{mat}_{3\alpha\beta} \Big[e_{\alpha\beta}(u)\, \partial_3\psi^{mat} - e_{\alpha\beta}(v)\, \partial_3\varphi^{mat} \Big]\, dx, \end{aligned}$$

for $mat = +, -$, *and*

$$l(v, \psi^+, \psi^-) = \int_\Omega f \cdot v\, dx + \int_{\Gamma_N^m} g \cdot v\, d\Gamma_N + \int_{\Omega^\pm} r\, \psi^\pm\, dx - \int_{\Gamma_{eN}^\pm} \theta\, \psi^\pm\, d\Gamma_{eN}^\pm.$$

In particular, u *is the asymptotic mechanical displacement in* Ω, φ^+ *and* φ^- *are the asymptotic electric potentials in* Ω^+ *and* Ω^-*; the triple* $(u, \varphi^+, \varphi^-)$ *is the unique solution of the variational equation* (13).

Proof: The proof is a straightforward extension of theorem 3.3 in [15], or equivalently and extension of problem (7) in [12] for a plate Ω made of one

elastic plate Ω^m and two piezoelectric patches Ω^- and Ω^+. We remark that the scalings used for the unknowns and data are those adopted in [15]. ■

Theorem 3.2. *Let us assume the electric boundary conditions* $(ebc1^{mat})$ *for both materials* $mat = +, -$. *Then, the asymptotic mechanical displacement* u *in* (13) *is the unique solution of the following variational problem, formulated in* Ω

$$\textit{find} \quad u \in V_{KL} \quad \textit{such that:} \qquad a(u,v) = l(v), \quad \forall v \in V_{KL}, \tag{14}$$

where $u_\alpha = \xi_\alpha - x_3 \partial_\alpha \xi_3$, *for* $\alpha = 1, 2$, $u_3 = \xi_3$,

$$\begin{aligned} a(u,v) \;=\; & \int_{\Omega^m} A^m_{\alpha\beta\gamma\rho} e_{\alpha\beta}(u) e_{\gamma\rho}(v)\, d\Omega^m + \int_{\Omega^-} A^-_{\alpha\beta\gamma\rho} e_{\alpha\beta}(u)\, e_{\gamma\rho}(v)\, d\Omega^- \\ & + \int_{\Omega^+} A^+_{\alpha\beta\gamma\rho} e_{\alpha\beta}(u)\, e_{\gamma\rho}(v)\, d\Omega^+ - \int_{\Omega^-} \frac{p^-_{3\alpha\beta} p^-_{3\gamma\rho}}{p^-_{33}} (x_3 - z^-)\, e_{\alpha\beta}(v)\, \partial_{\gamma\rho}\xi_3\, d\Omega^- \\ & - \int_{\Omega^+} \frac{p^+_{3\alpha\beta} p^+_{3\gamma\rho}}{p^+_{33}} (x_3 - z^+)\, e_{\alpha\beta}(v)\, \partial_{\gamma\rho}\xi_3\, d\Omega^+, \end{aligned} \tag{15}$$

and

$$\begin{aligned} l(v) \;=\; & \int_\Omega f \cdot v\, d\Omega + \int_{\Gamma_N} g \cdot v\, d\Gamma_N + \int_{\Omega^-} \left(\frac{P_3 r}{p^-_{33}} + \frac{(\varphi^-_{0lo} - \varphi^-_{0up} - R^-)}{t^-} \right) p^-_{3\alpha\beta}\, e_{\alpha\beta}(v)\, d\Omega^- \\ & + \int_{\Omega^+} \left(\frac{P_3 r}{p^+_{33}} + \frac{(\varphi^+_{0lo} - \varphi^+_{0up} - R^+)}{t^+} \right) p^+_{3\alpha\beta}\, e_{\alpha\beta}(v)\, d\Omega^+. \end{aligned} \tag{16}$$

Here φ^{mat}_{0up} *and* φ^{mat}_{0lo}, *with* $mat = +, -$, *are the restrictions of* φ^{mat}_0 *to, respectively, the upper and lower faces* Γ^{mat}_{up} *and* Γ^{mat}_{lo} *of* Ω^{mat}, *and* $R^{mat} := \int_{z^{mat} - \frac{t^{mat}}{2}}^{z^- + \frac{t^{mat}}{2}} \frac{P_3 r}{p^{mat}_{33}} dx_3$, *with* $P_3 r = \int r\, dy_3$ *the antiderivative of* r *with respect to the thickness variable* x_3. *In addition in* (13), *the asymptotic electrical potentials* φ^{mat} *(for* $mat = +, -$*) are defined by*

$$\begin{aligned} & \varphi^{mat}(x_1, x_2, x_3) = \varphi^{mat}_{0lo}(x_1, x_2) + \\ & \qquad \int_{z^{mat} - \frac{t^{mat}}{2}}^{x_3} \Big(- \frac{p^{mat}_{3\alpha\beta}}{p^{mat}_{33}} (y_3 - z^{mat})\, \partial_{\alpha\beta}\xi_3 + \frac{(\varphi^{mat}_{0up} - \varphi^{mat}_{0lo} + R^{mat})}{t^{mat}} - \frac{P_3 r}{p^{mat}_{33}} \Big)\, dy_3. \end{aligned} \tag{17}$$

Moreover, the bilinear form $a(u,v)$ *in (15) can be rewritten as*

$$a(u,v) = \int_\omega \Big[N_{\alpha\beta}(u)\, e_{\alpha\beta}(\eta) + M_{\alpha\beta}(u)\, \partial_{\alpha\beta}\eta_3 \Big]\, d\omega. \tag{18}$$

Here $(N_{\alpha\beta}(u))$ *and* $(M_{\alpha\beta}(u))$ *are the components of second-order tensor fields, associated to the Kirchhoff-Love displacement* u, *and given by the following*

matrix formula

$$\begin{bmatrix} N_{\alpha\beta}(u) \\ M_{\alpha\beta}(u) \end{bmatrix} = \begin{bmatrix} (A_0^m + A_0^+ + A_0^-)_{\alpha\beta\gamma\rho} & -(A_1^m + A_1^+ + A_1^-)_{\alpha\beta\gamma\rho} \\ -(A_1^m + A_1^+ + A_1^-)_{\alpha\beta\gamma\rho} & (A_2^m + A_2^+ + A_2^- + p_2^+ + p_2^-)_{\alpha\beta\gamma\rho} \end{bmatrix} \begin{bmatrix} e_{\gamma\rho}(\xi) \\ \partial_{\gamma\rho}\xi_3 \end{bmatrix}. \tag{19}$$

The matrices A_i^{mat}, p_j^{mat} (for $i = 0, 1, 2$, $j = 1, 2$, $mat = -, m, +$) are defined in (1)-(2), and $\xi = (\xi_1, \xi_2, \xi_3)$.

Proof: The proof is a straightforward extension of theorem 2.1 in [12], which itself is a generalization of of theorem 3.4 in [15] and consequently of theorem 3.1 in [25]. In fact, choosing in (13) $(\psi^+, \psi^-) = (0, 0)$ and using $(ebc1^{mat})$ for $mat = +, -$ we obtain the formula (17). Afterwards inserting these formulas in (13) we immediately get (15) and (16). To obtain the new formula (18) for the bilinear form it is enough to remark that in (15) $e_{\alpha\beta}(u) = e_{\alpha\beta}(\xi) - x_3\partial_{\alpha\beta}\xi_3$ and $e_{\alpha\beta}(v) = e_{\alpha\beta}(\eta) - x_3\partial_{\alpha\beta}\eta_3$. ∎

Corollary 3.1. *In addition to the conditions of theorem 3.2 we suppose both patches are made of the same piezoelectric material, have the same geometry, and are placed in symmetrical positions. Moreover, there are not any applied body and surface forces, and applied volume electric charge ($f = 0$, $g = 0$, $r = 0$). We also assume that the applied electric potential differences, $\varphi_{0lo}^{mat} - \varphi_{0up}^{mat}$, for $mat = +, -$, are equal or symmetrical. i) If $\varphi_{0lo}^+ - \varphi_{0up}^+ = -\big(\varphi_{0lo}^- - \varphi_{0up}^-\big)$, then the system (14) is equivalent to*

$$\int_\omega e_{\alpha\beta}(\eta)\,(A_0^m + A_0^+ + A_0^-)_{\alpha\beta\gamma\rho}\,e_{\gamma\rho}(\xi)\,d\omega = 0$$

$$\int_\omega \partial_{\alpha\beta}\eta_3\,(A_2^m + A_2^+ + A_2^- + p_2^+ + p_2^-)_{\alpha\beta\gamma\rho}\,\partial_{\gamma\rho}\xi_3\,d\omega = \int_{\omega^+} 2\big(\varphi_{0lo}^+ - \varphi_{0up}^+\big)\,p_{3\alpha\beta}^+ z^+\,\partial_{\alpha\beta}\eta_3\,d\omega^+$$

which means the tangential mechanical displacements $\xi_1 = \xi_2 = 0$. ii) If $\varphi_{0lo}^+ - \varphi_{0up}^+ = \varphi_{0lo}^- - \varphi_{0up}^-$, then (14) is equivalent to

$$\begin{cases} \int_\omega e_{\alpha\beta}(\eta)\,(A_m^0)_{\alpha\beta\gamma\rho}\,e_{\gamma\rho}(\xi)\,d\omega = \int_{\omega^+} 2\left(\varphi_{0lo}^+ - \varphi_{0up}^+\right)p_{3\alpha\beta}^+\,e_{\alpha\beta}(\eta)\,d\omega^+ \\ \int_\omega \partial_{\alpha\beta}\eta_3\,(A_2^m + A_2^+ + A_2^- + p_2^+ + p_2^-)_{\alpha\beta\gamma\rho}\,\partial_{\gamma\rho}\xi_3\,d\omega = 0, \end{cases}$$

and in this case the transverse mechanical displacement $\xi_3 = 0$.

Proof: With the material and geometric hypotheses imposed to the patches we have that $\omega^+ = \omega^-$, $z^m = 0$, $z^- = -z^+$ and $t^- = t^+$. Therefore, the

matrix in the right hand side of (19) becomes

$$\left[\begin{array}{cc} (A_0^m + A_0^+ + A_0^-)_{\alpha\beta\gamma\rho} & 0 \\ 0 & (A_2^m + A_2^+ + A_2^- + p_2^+ + p_2^-)_{\alpha\beta\gamma\rho} \end{array}\right]$$

and the linear form in (16) is now equal to

$$l(v) = \left\{ \begin{array}{l} \int_{\omega^+} 2\left(\varphi_{0lo}^+ - \varphi_{0up}^+\right) p_{3\alpha\beta}^+ \, z^+ \, \partial_{\alpha\beta}\eta_3 \, d\omega^+, \quad \text{when} \quad \varphi_{0lo}^+ - \varphi_{0up}^+ = -\left(\varphi_{0lo}^- - \varphi_{0up}^-\right) \\ \int_{\omega^+} 2\left(\varphi_{0lo}^+ - \varphi_{0up}^+\right) p_{3\alpha\beta}^+ \, e_{\alpha\beta}(\eta) \, d\omega^+, \quad \text{when} \quad \varphi_{0lo}^+ - \varphi_{0up}^+ = \varphi_{0lo}^- - \varphi_{0up}^- \end{array} \right.$$

This gives the result. ∎

Theorem 3.3. *Let us assume the electric boundary conditions* $(ebc2^{mat})$ *or* $(ebc3^{mat})$ *for both materials* $mat = +, -$. *Then, the asymptotic mechanical displacement* u *in* (13) *is the unique solution of the following variational problem, formulated in* Ω

$$\textit{find} \quad u \in V_{KL} \quad \textit{such that:} \qquad a(u,v) = l(v), \quad \forall v \in V_{KL}, \tag{20}$$

where $u_\alpha = \xi_\alpha - x_3 \partial_\alpha \xi_3$, *for* $\alpha = 1, 2$, $u_3 = \xi_3$

$$\begin{array}{rcl} a(u,v) & = & \int_{\Omega^m} A_{\alpha\beta\gamma\rho}^m e_{\alpha\beta}(u) e_{\gamma\rho}(v) \, d\Omega^m + \int_{\Omega^-} A_{\alpha\beta\gamma\rho}^- e_{\alpha\beta}(u) \, e_{\gamma\rho}(v) \, d\Omega^- \\ & & + \int_{\Omega^+} A_{\alpha\beta\gamma\rho}^+ e_{\alpha\beta}(u) \, e_{\gamma\rho}(v) \, d\Omega^+ + \int_{\Omega^-} \frac{p_{3\alpha\beta}^- p_{3\gamma\rho}^-}{p_{33}^-} \, e_{\alpha\beta}(u) \, e_{\alpha\beta}(v) \, d\Omega^- \\ & & + \int_{\Omega^+} \frac{p_{3\alpha\beta}^+ p_{3\gamma\rho}^+}{p_{33}^+} \, e_{\alpha\beta}(u) \, e_{\alpha\beta}(v) \, d\Omega^+, \end{array} \tag{21}$$

and

$$l(v) = \int_\Omega f \cdot v \, d\Omega + \int_{\Gamma_N} g \cdot v \, d\Gamma_N + l^{ebci^+}(v) + l^{ebci^-}(v),$$

where for $mat = +, -$

$$l^{ebci^{mat}}(v) = \int_{\Omega^{mat}} \frac{p_{3\alpha\beta}^{mat}}{p_{33}^{mat}} \left[P_3 r(x_1, x_2, x_3) + (s\,\theta - P_3 r)(x_1, x_2, h^*) \right] e_{\alpha\beta}(v).$$

Here $s = 1$ *and* $h^* = z^{mat} + \frac{t^{mat}}{2}$ *for* $(ebc2^{mat})$, $s = -1$ *and* $h^* = z^{mat} - \frac{t^{mat}}{2}$ *for* $(ebc3^{mat})$. *The asymptotic electrical potential* φ^{mat} *in* Ω^{mat}, *for* $mat = +, -$, *is defined by*

$$\begin{array}{rcl} \varphi^{mat}(x_1, x_2, x_3) & = & \varphi_{0lo}^{mat}(x_1, x_2) + \int_{z^{mat} - \frac{t^{mat}}{2}}^{x_3} \frac{p_{3\alpha\beta}^{mat}}{p_{33}^{mat}} \left[e_{\alpha\beta}(\xi) - y_3 \, \partial_{\alpha\beta}\xi_3 \right] dy_3 \\ & & - \int_{z^{mat} - \frac{t^{mat}}{2}}^{x_3} \frac{P_3 r(x_1, x_2, y_3) + (\theta - P_3 r)(x_1, x_2, z^{mat} + \frac{t^{mat}}{2})}{p_{33}^{mat}} \, dy_3, \end{array}$$

for $(ebc2^{mat})$ *and by*

$$\varphi^{mat}(x_1,x_2,x_3) = \varphi^{mat}_{0up}(x_1,x_2) - \int_{x_3}^{z^{mat}+\frac{t^{mat}}{2}} \frac{p^{mat}_{3\alpha\beta}}{p^{mat}_{33}} \left[e_{\alpha\beta}(\xi) - y_3\,\partial_{\alpha\beta}\xi_3\right] dy_3 + \int_{x_3}^{z^{mat}+\frac{t^{mat}}{2}} \frac{P_3 r(x_1,x_2,y_3)+(-\theta-P_3 r)(x_1,x_2,z^{mat}-\frac{t^{mat}}{2})}{p^{mat}_{33}}\, dy_3,$$

for $(ebc3^{mat})$. *Moreover, the bilinear form* $a(u,v)$ *in* (21) *can be rewritten as*

$$a(u,v) = \int_\omega \Big[N_{\alpha\beta}(u)\, e_{\alpha\beta}(\eta) + M_{\alpha\beta}(u)\,\partial_{\alpha\beta}\eta_3\Big]\, d\omega,$$

where $(N_{\alpha\beta}(u))$ *and* $(M_{\alpha\beta}(u))$ *are the components of second-order tensor fields associated to the Kirchhoff-Love displacement* u *given by the following matrix formula*

$$\begin{bmatrix} N_{\alpha\beta}(u) \\ M_{\alpha\beta}(u) \end{bmatrix} = \begin{bmatrix} (A_0^m + A_0^+ + A_0^- + pp_0^+ + pp_0^-)_{\alpha\beta\gamma\rho} & -(A_1^m + A_1^+ + A_1^- + pp_1^+ + pp_1^-)_{\alpha\beta\gamma\rho} \\ -(A_1^m + A_1^+ + A_1^- + pp_1^+ + pp_1^-)_{\alpha\beta\gamma\rho} & (A_2^m + A_2^+ + A_2^- + pp_2^+ + pp_2^-)_{\alpha\beta\gamma\rho} \end{bmatrix} \begin{bmatrix} e_{\gamma\rho}(\xi) \\ \partial_{\gamma\rho}\xi_3 \end{bmatrix}.$$

The matrices A_i^{mat} *and* p_j^{mat}, *with* $i=0,1,2$, $j=1,2$ *and for* $mat=-,m,+$, *are defined in (1)-(2), and* $\xi=(\xi_1,\xi_2,\xi_3)$.

Proof: The proof is a combination of the results found in section 3.4 of [17] for the electric potentials together with the new geometry of the plate $\Omega = \Omega^+ \cup \Omega^m \cup \Omega^-$. ∎

Corollary 3.2. *In addition to the conditions of theorem 3.3 we suppose both patches verify* $(ebc2^{mat})$, *are made of the same piezoelectric material, have the same geometry, are placed in symmetrical positions. Moreover, there are not any applied body and surface forces, and applied volume electric charge* ($f=0$, $g=0$, $r=0$). *We assume that the applied surface electric charges* θ^+ *and* θ^- *acting on* Γ^+_{eN} *and* Γ^-_{eN}, *respectively, are equal or symmetrical. i) If* $\theta^+ = -\theta^- = \theta$, *then the system* (20) *is equivalent to*

$$\begin{cases} \int_\omega e_{\alpha\beta}(\eta)\,(A_m^0 + A_0^+ + A_0^- + pp_0^+ + pp_0^-)_{\alpha\beta\gamma\rho}\, e_{\gamma\rho}(\xi)\, d\omega = 0 \\ \int_\omega \partial_{\alpha\beta}\eta_3\,(A_2^m + A_2^+ + A_2^- + pp_2^+ + pp_2^-)_{\alpha\beta\gamma\rho}\,\partial_{\gamma\rho}\xi_3\, d\omega = -s\int_{\omega^+} 2\,\frac{p^+_{3\alpha\beta}}{p^+_{33}}\,(\theta\, t^+ z^+)\,\partial_{\alpha\beta}\eta_3\, d\omega^+, \end{cases}$$

which means the tangential mechanical displacements $\xi_1 = \xi_2 = 0$. *ii) If* $\theta^+ = \theta^- = \theta$, *then* (20) *is equivalent to*

$$\begin{cases} \int_\omega e_{\alpha\beta}(\eta)\,(A_m^0 + A_0^+ + A_0^- + pp_0^+ + pp_0^-)_{\alpha\beta\gamma\rho}\, e_{\gamma\rho}(\xi)\,d\omega = s\int_{\omega^+} 2\,t^+\,\frac{p^+_{3\alpha\beta}}{p^+_{33}}\,\theta\, e_{\alpha\beta}(\eta)\,d\omega^+ \\ \int_\omega \partial_{\alpha\beta}\eta_3\,(A_2^m + A_2^+ + A_2^- + pp_2^+ + pp_2^-)_{\alpha\beta\gamma\rho}\,\partial_{\gamma\rho}\xi_3\,d\omega = 0, \end{cases}$$

and in this case the transverse mechanical displacement $\xi_3 = 0$.

Proof: Analogous to that of corollary 3.1. A similar result applies if both patches verify electric boundary conditions ($ebc3^{mat}$). ■

4. Plate with an inserted patch – PIP

The procedure is the same as indicated at the beginning of section 3, but now for the PIP structure. The asymptotic models are stated in theorems 4.1, 4.2 and 4.3.

4.1. The three-dimensional model – PIP. We consider a three-dimensional thin plate $\Omega = \cup_{mat}\Omega^{mat}$ with thickness $2h$, made of two external elastic layers (Ω^- on the bottom and Ω^+ on the top of the structure) and an internal layer which includes and elastic part Ω^e and an inserted piezoelectric patch Ω^p. This means that the subscript *mat* ranges now the set $\{-, e, p, +\}$, $\Omega = \Omega^- \cup \Omega^m \cup \Omega^+$ with $\Omega^m = \omega^m \times (z^m - \frac{t^m}{2}, z^m + \frac{t^m}{2}) = \Omega^p \cup \Omega^e$ and

$$\begin{aligned} &\Omega^- = \omega^- \times (z^- - \tfrac{t^-}{2}, z^- + \tfrac{t^-}{2}), \\ &\Omega^p = \omega^p \times (z^p - \tfrac{t^p}{2}, z^p + \tfrac{t^p}{2}), \\ &\Omega^e = \omega^e \times (z^e - \tfrac{t^e}{2}, z^e + \tfrac{t^e}{2}), \quad \omega^e = \omega^m \setminus \omega^p \\ &\Omega^+ = \omega^+ \times (z^+ - \tfrac{t^+}{2}, z^+ + \tfrac{t^+}{2}). \end{aligned} \tag{22}$$

The positive scalars t^-, t^e, t^p and t^+, with $t^e = t^p = t^m$, represent the thicknesses of layers Ω^-, Ω^e, Ω^p and Ω^+, respectively, and verify $t^- + t^m + t^+ = 2h$. The absolute values $|z^-|$, $|z^e|$, $|z^p|$ and $|z^+|$, with $z^e = z^p = z^m$, are the

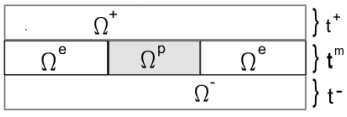

FIGURE 2. Vertical cross section along the thickness for a sandwich elastic rectangular plate with an inserted piezoelectric patch

distances, measured along the thickness axis, from the middle plane of Ω to the middle plane of layers Ω^-, Ω^m and Ω^+, respectively. The geometrical and

material properties of the three elastic parts and the piezoelectric patch are indexed by the upper subscripts $-$ or $+$ for the lower or upper layers, and by e or p for the internal elastic layer and inserted piezoelectric patch.

We define the following boundary sets of Ω^p and also two disjoint parts, Γ_D, Γ_N, of the boundary of Ω by

$$\begin{aligned}
&\Gamma^p_{up/lo} = \Gamma^p_{lo} \cup \Gamma^p_{up}, \quad \Gamma^p_{lo} = \omega^p \times \{z^p - \tfrac{t^p}{2}\}, \quad \Gamma^p_{up} = \omega^p \times \{z^p + \tfrac{t^p}{2}\},\\
&\Gamma^p_s = \gamma^p_s \times (z^p - \tfrac{t^p}{2}, z^p + \tfrac{t^p}{2}),\\
&\Gamma^p_e = \gamma^p_e \times (z^p - \tfrac{t^p}{2}, z^p + \tfrac{t^p}{2}),\\
&\Gamma_D = \gamma_0 \times (-h, +h), \qquad\qquad \Gamma_N = \Gamma \setminus \Gamma_D.
\end{aligned} \tag{23}$$

We consider three different disjoint partitions $\{\Gamma^p_{eD}, \Gamma^p_{eN}\}$ of the boundary of Ω^p defined by

$$\begin{aligned}
&(ebc1^p): \quad \Gamma^p_{eN} = \Gamma^p_s \quad \text{and} \quad \Gamma^p_{eD} = \Gamma^p_{up/lo} \cup \Gamma^p_e\\
&(ebc2^p): \quad \Gamma^p_{eN} = \Gamma^p_s \cup \Gamma^p_{up} \quad \text{and} \quad \Gamma^p_{eD} = \Gamma^p_{lo} \cup \Gamma^p_e\\
&(ebc3^p): \quad \Gamma^p_{eN} = \Gamma^p_s \cup \Gamma^p_{lo} \quad \text{and} \quad \Gamma^p_{eD} = \Gamma^p_{up} \cup \Gamma^p_e
\end{aligned} \tag{24}$$

Now the three-dimensional model, corresponding to the mechanical and electric equilibrium state of the structure PIP, aims to find the mechanical displacement u defined in $\Omega = \Omega^- \cup \Omega^m \cup \Omega^+$ and the electric potential φ defined in Ω^p, satisfying the following system of equations and boundary conditions (25)–(29):

$$\left[\begin{array}{ll} -\operatorname{div}\sigma = f & \text{in} \quad \Omega = \Omega^- \cup \Omega^m \cup \Omega^+\\ \operatorname{div} D = r & \text{in} \quad \Omega^p, \end{array}\right. \tag{25}$$

$$u = 0 \quad \text{on} \quad \Gamma_D \quad \text{and} \quad \sigma \cdot \nu = g \quad \text{on} \quad \Gamma_N, \tag{26}$$

$$\left[\begin{array}{ll} D \cdot \nu = \theta & \text{on} \quad \Gamma^p_{eN}\\ \varphi = \varphi_0 & \text{on} \quad \Gamma^p_{eD}, \end{array}\right. \tag{27}$$

$$\begin{aligned}
&u^p = u^- \quad \text{and} \quad (\sigma^p - \sigma^-)\cdot\nu = 0, \quad \text{on} \quad \Omega^- \cap \Omega^p = \omega^p \times \{z^p - \tfrac{t^p}{2}\}\\
&u^p = u^+ \quad \text{and} \quad (\sigma^p - \sigma^+)\cdot\nu = 0 \quad \text{on} \quad \Omega^+ \cap \Omega^p = \omega^p \times \{z^p + \tfrac{t^p}{2}\}\\
&u^e = u^- \quad \text{and} \quad (\sigma^e - \sigma^-)\cdot\nu = 0 \quad \text{on} \quad \Omega^- \cap \Omega^e = \omega^e \times \{z^e - \tfrac{t^e}{2}\}\\
&u^e = u^+ \quad \text{and} \quad (\sigma^e - \sigma^+)\cdot\nu = 0 \quad \text{on} \quad \Omega^+ \cap \Omega^e = \omega^e \times \{z^e + \tfrac{t^e}{2}\},\\
&u^e = u^p \quad \text{and} \quad (\sigma^e - \sigma^p)\cdot\nu = 0 \quad \text{on} \quad \Omega^e \cap \Omega^p = \partial\omega^p \times (z^m - \tfrac{t^m}{2}, z^m + \tfrac{t^m}{2}),
\end{aligned} \tag{28}$$

$$\begin{aligned}
&\sigma = C^e \cdot e(u) \quad \text{in } \Omega^e\\
&\sigma = C^- \cdot e(u) \quad \text{in } \Omega^-\\
&\sigma = C^+ \cdot e(u) \quad \text{in } \Omega^+
\end{aligned}
\qquad \text{and} \qquad
\left[\begin{array}{l} \sigma = C^p \cdot e(u) - P^p \cdot E(\varphi)\\ D = P^p \cdot e(u) + \varepsilon^p \cdot E(\varphi) \end{array}\right. \quad \text{in } \Omega^p. \tag{29}$$

These equations have a similar interpretation to that given for (8)–(12). We repeat it here for the sake of convenience of the reading. The equations (25) are the mechanical equilibrium equations and Maxwell-Gauss equations, with σ the stress tensor field, D the electric displacement vector field and f and r are the density of the applied body forces and volume electric charge acting on the plate Ω. The mechanical boundary conditions are defined by (26), and impose that the plate is clamped on Γ_D and submitted to the density of applied surface forces g on Γ_N. The electric boundary conditions are stated in (27) and mean that the plate is submitted to the applied electric potential φ_0 on Γ^p_{eD}, and subject to a surface electric charge on Γ^p_{eN} of density θ. The equations (28) are the transmission conditions at the interfaces. Finally (29) are the constitutive equations, where C^p, C^e, C^- and C^+ are the elasticity tensors for the different materials, and P^p and ε^p are the piezoelectric and dielectric tensors of the piezoelectric patch.

4.2. The asymptotic model – PIP.

Theorem 4.1. *Let V_{KL}, Ψ^p_l and Ψ^p_{l0} be the admissible spaces defined in (4) with mat = p. Then, the variational asymptotic model corresponding to problem* (25)-(29) *is*

$$\left\{\begin{array}{l} \textit{Find} \quad (u,\varphi^p)\in V_{KL}\times\Psi^p_l \quad \textit{such that:} \\ a\Big((u,\varphi^p),(v,\psi^p)\Big)=l(v,\psi^p), \quad \forall (v,\psi^p)\in V_{KL}\times\Psi^p_{l0}, \\ \varphi=\varphi_0, \quad \textit{on} \quad \Gamma^p_{eD}, \end{array}\right. \tag{30}$$

where

$$a\Big((u,\varphi^p),(v,\psi^p)\Big)=a^e(u,v)+a^+(u,v)+a^-(u,v)+a^p\Big((u,\varphi^p),(v,\psi^p)\Big)$$

$$a^{mat}(u,v)=\int_{\Omega^{mat}} A^{mat}_{\alpha\beta\gamma\rho}e_{\alpha\beta}(u)e_{\gamma\rho}(v)\,dx, \quad \textit{for mat} = e,+,-$$

$$\begin{aligned} a^p\Big((u,\varphi^p),(v,\psi^p)\Big) \;=\; & \textstyle\int_{\Omega^p} A^p_{\alpha\beta\gamma\rho}e_{\alpha\beta}(u)e_{\gamma\rho}(v)\,dx+\int_{\Omega^p} p^p_{33}\,\partial_3\varphi^p\,\partial_3\psi^p\,dx \\ & -\textstyle\int_{\Omega^p} p^p_{3\alpha\beta}\Big[e_{\alpha\beta}(u)\partial_3\psi^p-e_{\alpha\beta}(v)\partial_3\varphi^p\Big]\,dx \end{aligned}$$

$$l(v,\psi^p)=\int_\Omega f\cdot v\,dx+\int_{\Gamma_N} g\cdot v\,d\Gamma_N+\int_{\Omega^p} r\,\psi^p\,dx-\int_{\Gamma^p_{eN}}\theta\,\psi^p\,d\Gamma^p_{eN}.$$

In particular, u is the asymptotic mechanical displacement, φ^p is the asymptotic electric potential in Ω^p (the pair (u,φ^p) is the unique solution of the variational equation (30)) and

Proof: Analogous to the proof of theorem 3.1. ∎

Theorem 4.2. *Let us assume the electric boundary conditions $(ebc1^p)$. The asymptotic mechanical displacement u in (30) is the unique solution of the following variational problem, formulated in Ω*

$$\textit{Find} \quad u \in V_{KL} \quad \textit{such that:} \qquad a(u,v) = l(v), \quad \forall v \in V_{KL},$$

where $u_\alpha = \xi_\alpha - x_3\partial_\alpha\xi_3$, for $\alpha = 1,2$, $u_3 = \xi_3$,

$$\begin{aligned} a(u,v) \;=\; & \textstyle\int_{\Omega^+} A^+_{\alpha\beta\gamma\rho} e_{\alpha\beta}(u) e_{\gamma\rho}(v)\, d\Omega^+ + \int_{\Omega^-} A^-_{\alpha\beta\gamma\rho} e_{\alpha\beta}(u) e_{\gamma\rho}(v)\, d\Omega^- \\ & + \textstyle\int_{\Omega^e} A^e_{\alpha\beta\gamma\rho} e_{\alpha\beta}(u) e_{\gamma\rho}(v)\, d\Omega^e + \int_{\Omega^p} A^p_{\alpha\beta\gamma\rho} e_{\alpha\beta}(u) e_{\gamma\rho}(v)\, d\Omega^p \\ & - \textstyle\int_{\Omega^p} \frac{p^p_{3\alpha\beta} p^p_{3\gamma\rho}}{p^p_{33}} \,(x_3 - z^m)\, e_{\alpha\beta}(v)\, \partial_{\gamma\rho}\xi_3 \, d\Omega^p, \end{aligned} \tag{31}$$

and

$$l(v) = \int_\Omega f\cdot v\, d\Omega + \int_{\Gamma_N} g\cdot v\, d\Gamma_N + \int_{\Omega^p} \Big(\frac{P_3 r}{p^p_{33}} + \frac{(\varphi_{0lo} - \varphi_{0up} - R^p)}{t^p} \Big)\, p^p_{3\alpha\beta}\, e_{\alpha\beta}(v)\, d\Omega^p. \tag{32}$$

Here φ_{0up} and φ_{0lo} are the restrictions of φ_0 to the upper and lower faces, Γ^p_{up} and Γ^p_{lo}, respectively, of Ω^p, and $R^p := \int_{z^p-\frac{t^p}{2}}^{z^p+\frac{t^p}{2}} \frac{P_3 r}{p^p_{33}} dx_3$ (see (16)). The asymptotic electrical potential φ in Ω^p is defined by

$$\varphi(x_1,x_2,x_3) = \varphi_{0lo}(x_1,x_2) + \int_{z^p-\frac{t^p}{2}}^{x_3} \Big(-\frac{p^p_{3\alpha\beta}}{p^p_{33}}\,(y_3 - z^p)\,\partial_{\alpha\beta}\zeta_3 + \frac{(\varphi_{0up} - \varphi_{0lo} + R^p)}{t^p} - \frac{P_3 r}{p^p_{33}} \Big)\, dy_3.$$

Moreover, the bilinear form $a(u,v)$ in (31) can be rewritten as

$$a(u,v) = \int_\omega \Big[N_{\alpha\beta}(u)\, e_{\alpha\beta}(\eta) + M_{\alpha\beta}(u)\, \partial_{\alpha\beta}\eta_3 \Big]\, d\omega,$$

with $(N_{\alpha\beta}(u))$ and $(M_{\alpha\beta}(u))$ given now by the following matrix formula

$$\begin{bmatrix} N_{\alpha\beta}(u) \\ M_{\alpha\beta}(u) \end{bmatrix} = \\ \begin{bmatrix} (A^p_0 + A^e_0 + A^+_0 + A^-_0)_{\alpha\beta\gamma\rho} & -(A^p_1 + A^e_1 + A^+_1 + A^-_1 + p^p_1)_{\alpha\beta\gamma\rho} \\ -(A^p_1 + A^e_1 + A^+_1 + A^-_1)_{\alpha\beta\gamma\rho} & (A^p_2 + A^e_2 + A^+_2 + A^-_2 + p^p_2)_{\alpha\beta\gamma\rho} \end{bmatrix} \begin{bmatrix} e_{\gamma\rho}(\xi) \\ \partial_{\gamma\rho}\xi_3 \end{bmatrix}, \tag{33}$$

where for $mat = -, e, p, +$ the matrices A^{mat}_i and p^p_j with $i = 0,1,2$ and $j = 1,2$ are defined in (1)-(2), and $\xi = (\xi_1,\xi_2,\xi_3)$.

Proof: Similar to the proof of theorem 3.2. ■

Corollary 4.1. *In addition to the conditions of theorem 4.2 we assume the two external layers, Ω^- and Ω^+, have the same geometry and are made of the same elastic material. i) If $\varphi_{0lo} = \varphi_{0up}$, $r = 0$, $f_1 = f_2 = 0$, $g = 0$ and $f_3 \neq 0$, then the mechanical displacements $\xi_1 = \xi_2 = 0$ and $\xi_3 \neq 0$. ii) If φ_{0lo}, φ_{0up} are independent of the thickness variable, $\varphi_{0lo} \neq \varphi_{0up}$, $r = 0$, $f = 0$, $g = 0$, then $\xi_3 = 0$ and $\xi_1 \neq 0 \neq \xi_2$.*

Proof: It is enough to remark that the matrix in the right hand side of (33) is equal to

$$\begin{bmatrix} (A_0^p + A_0^e + A_0^+ + A_0^-)_{\alpha\beta\gamma\rho} & 0 \\ 0 & (A_2^p + A_2^e + A_2^+ + A_2^- + p_2^p)_{\alpha\beta\gamma\rho} \end{bmatrix}$$

and the linear form in (32) is equal to

$$l(v) = \begin{cases} \int_\Omega f_3 \cdot v_3 \, d\Omega, & \text{with the hypotheses i)} \\ \int_{\Omega^p} \frac{(\varphi_{0lo} - \varphi_{0up})}{t^p} \, p^p_{3\alpha\beta} \, e_{\alpha\beta}(v) \, d\Omega^p, & \text{with the hypotheses ii).} \end{cases}$$

■

Theorem 4.3. *Let us assume the electric boundary conditions $(ebc2^p)$ or $(ebc3^p)$. Then, the asymptotic mechanical displacement u in (30) is the unique solution of the following variational problem, formulated in Ω*

$$\text{find} \quad u \in V_{KL} \quad \text{such that:} \qquad a(u,v) = l(v), \quad \forall v \in V_{KL}, \tag{34}$$

where $u_\alpha = \xi_\alpha - x_3 \partial_\alpha \xi_3$, for $\alpha = 1, 2$, $u_3 = \xi_3$

$$\begin{aligned} a(u,v) \;=\; & \int_{\Omega^+} A^+_{\alpha\beta\gamma\rho} e_{\alpha\beta}(u) e_{\gamma\rho}(v) \, d\Omega^+ + \int_{\Omega^-} A^-_{\alpha\beta\gamma\rho} e_{\alpha\beta}(u) e_{\gamma\rho}(v) \, d\Omega^- \\ & + \int_{\Omega^e} A^e_{\alpha\beta\gamma\rho} e_{\alpha\beta}(u) e_{\gamma\rho}(v) \, d\Omega^e + \int_{\Omega^p} A^p_{\alpha\beta\gamma\rho} e_{\alpha\beta}(u) \, e_{\gamma\rho}(v) \, d\Omega^p \\ & + \int_{\Omega^p} \frac{p^p_{3\alpha\beta} p^p_{3\gamma\rho}}{p^p_{33}} \, e_{\alpha\beta}(u) \, e_{\alpha\beta}(v) \, d\Omega^p, \end{aligned} \tag{35}$$

and

$$l(v) = \int_\Omega f \cdot v \, d\Omega + \int_{\Gamma_N} g \cdot v \, d\Gamma_N + l^{ebci^p}(v),$$

where

$$l^{ebci^p}(v) = \int_{\Omega^p} \frac{p^p_{3\alpha\beta}}{p^p_{33}} \big[P_3 r(x_1, x_2, x_3) + (s\,\theta - P_3 r)(x_1, x_2, h^*) \big] \, e_{\alpha\beta}(v).$$

Here $s = 1$ *and* $h^* = z^p + \frac{t^p}{2}$ *for* $(ebc2^p)$, $s = -1$ *and* $h^* = z^p - \frac{t^p}{2}$ *for* $(ebc3^p)$. *The asymptotic electrical potential* φ^p *in* Ω^p, *is defined by*

$$\begin{aligned}\varphi^p(x_1,x_2,x_3) &= \varphi_{0lo}(x_1,x_2) + \int_{z^p-\frac{t^p}{2}}^{x_3} \frac{p^p_{3\alpha\beta}}{p^p_{33}}\left[e_{\alpha\beta}(\xi) - y_3\,\partial_{\alpha\beta}\xi_3\right] dy_3 \\ &\quad - \int_{z^p-\frac{t^p}{2}}^{x_3} \frac{P_3 r(x_1,x_2,y_3)+(\theta-P_3 r)(x_1,x_2,z^p+\frac{t^p}{2})}{p^p_{33}}\, dy_3,\end{aligned}$$

for $(ebc2^p)$ *and by*

$$\begin{aligned}\varphi^p(x_1,x_2,x_3) &= \varphi_{0up}(x_1,x_2) - \int_{x_3}^{z^p+\frac{t^p}{2}} \frac{p^p_{3\alpha\beta}}{p^p_{33}}\left[e_{\alpha\beta}(\xi) - y_3\,\partial_{\alpha\beta}\xi_3\right] dy_3 \\ &\quad + \int_{x_3}^{z^p+\frac{t^p}{2}} \frac{P_3 r(x_1,x_2,y_3)+(-\theta-P_3 r)(x_1,x_2,z^p-\frac{t^p}{2})}{p^p_{33}}\, dy_3,\end{aligned}$$

for $(ebc3^p)$. *Moreover, the bilinear form* $a(u,v)$ *in in* (35) *can be rewritten as*

$$a(u,v) = \int_\omega \Big[N_{\alpha\beta}(u)\, e_{\alpha\beta}(\eta) + M_{\alpha\beta}(u)\,\partial_{\alpha\beta}\eta_3\Big]\, d\omega,$$

where $(N_{\alpha\beta}(u))$ *and* $(M_{\alpha\beta}(u))$ *are now given by the following matrix formula*

$$\begin{bmatrix} N_{\alpha\beta\gamma\rho}(u) \\ M_{\alpha\beta\gamma\rho}(u) \end{bmatrix} =$$

$$\begin{bmatrix} (A_0^p + A_0^e + A_0^+ + A_0^- + pp_0^p)_{\alpha\beta\gamma\rho} & -(A_1^p + A_1^e + A_1^+ + A_1^- + pp_1^p)_{\alpha\beta\gamma\rho} \\ -(A_1^p + A_1^e + A_1^+ + A_1^- + pp_1^p)_{\alpha\beta\gamma\rho} & (A_2^p + A_2^e + A_2^+ + A_2^- + pp_2^p)_{\alpha\beta\gamma\rho} \end{bmatrix} \begin{bmatrix} e_{\gamma\rho}(\xi) \\ \partial_{\gamma\rho}\xi_3 \end{bmatrix}.$$

Here the matrices A_i^{mat} *and* pp_p^{mat}, *with* $i = 0,1,2$, $j = 1,2$ *and for* $mat = -, p, e, +$, *are defined in (1)-(2), and* $\xi = (\xi_1,\xi_2,\xi_3)$.

Proof: Similar to the proof of theorem 3.3. ∎

Corollary 4.2. *In addition to the conditions of theorem 4.3 we assume the inserted patch verifies* $(ebc2^p)$, *the two external layers,* Ω^- *and* Ω^+, *have the same geometry and are made of the same elastic material. i) If* $\theta = 0$, $r = 0$, $f_1 = f_2 = 0$, $g = 0$ *and* $f_3 \neq 0$, *then tangential mechanical displacements* $\xi_1 = \xi_2 = 0$ *and* $\xi_3 \neq 0$. *ii) If* θ *is independent of the thickness variable, and not zero, and* $r =$, $f = 0$, $g = 0$, *then* $\xi_1 \neq 0 \neq \xi_2$ *and* $\xi_3 = 0$.

Proof: Similar to the proof of corollary 4.1. An analogous result exists if the inserted patch verifies $(ebc3^p)$. ∎

5. Numerical simulations

In this section we report the numerical tests done with the asymptotic models described in sections 3 and 4 for elastic plates with two surface bonded piezoelectric patches (PSBP) or with one inserted piezoelectric patch (PIP). All the tests where executed with the software COMSOL MULTIPHYSICS® [11]. We use Lagrange shape functions of degree 1 and Hermite shape functions of degree 3, for the finite element discretization of the Kirchhoff-Love mechanical tangential displacements ξ_1, ξ_2 and ξ_3, respectively.

For both structures, either PSBP or PIP, the elastic material is always Graphite Epoxy 0^0 and the patches are made of the same PZT piezoelectric ceramic material. The values of the material parameters are taken from the tables VIII and XI in [19].

In all our examples we consider $\omega = [0, 0.5] \times [0, 0.25]$ for the middle plane of the structure, and $t^m = 0.015$, $t^+ = 0.005$, $t^- = 0.005$ and $t^p = 0.015$, for the thicknesses of the middle elastic plate, the upper and lower layer or patch, and the thickness of the inserted patch, respectively. Moreover, we consider a triangular finite element mesh with 498 elements in ω. Unless otherwise stated the applied body forces, surface forces and volume electric charge densities, f, g and r, are zero. The data are given in SI units, i.e., length is measured in meter, mechanical forces in Newton and electrical potentials in Volt.

The Figure 3 illustrates, for a plate of type PSBP verifying the hypotheses of corollary 3.1, the influence of the clamped mechanical boundary conditions on the mechanical displacements: when the plate is clamped in one side (top row), two consecutive sides (middle row) and three sides (bottom row). The projections of the piezoelectric patches on the middle plane of the plate are $\omega^+ = \omega^- = [0, 0.5] \times [0.25/9, 2 * 0.25/9]$ and the two patches satisfy electric boundary conditions $(ebc1^{mat})$. For the left column the data correspond to assumptions i) of corollary 3.1 (consequently $\xi_1 = 0 = \xi_2$) and it shows the transverse displacements ξ_3 of the middle plane of this plate; here $\varphi^+_{0lo} - \varphi^+_{0up} = -\big(\varphi^-_{0lo} - \varphi^-_{0up}\big) = -100$, with $\varphi^+_{0up} = 100$, $\varphi^-_{0lo} = 100$. For the right column the data are consistent with the assumptions ii) of corollary 3.1 (thus $\xi_3 = 0$), and it depicts the deformed middle plane of the plate (multiplied by 10^4 and in the tangential directions x_1, x_2); for this case $\varphi^+_{0lo} - \varphi^+_{0up} = \varphi^-_{0lo} - \varphi^-_{0up} = 100$, with $\varphi^+_{0lo} = 100$, $\varphi^-_{0lo} = 100$.

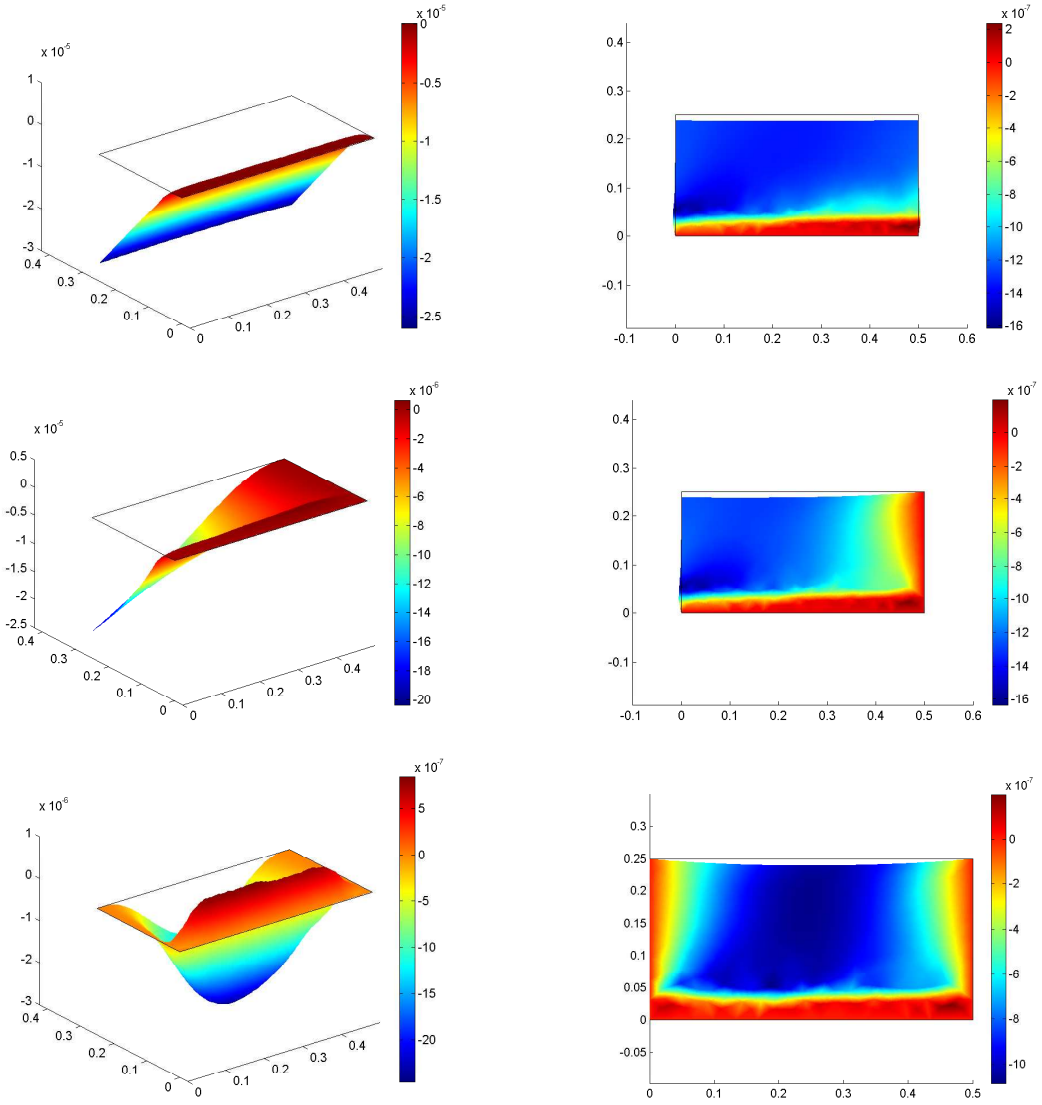

FIGURE 3. Elastic plate with two bonded surface piezoelectric patches (PSBP), verifying the conditions of corollary 3.1, and three different clamped mechanical boundary conditions. Left column: transverse displacements ξ_3 (the plate verifies assumptions i) of corollary 3.1). Right column: deformed middle plane (multiplied by 10^4) of the plate in the tangential directions (the plate verifies assumptions ii) of corollary 3.1). The plate is clamped in one side (top row), in two consecutive sides (middle row) and in three sides (bottom row).

The Figure 4 concerns two plates of type PSBP, and gives information about the significant differences originated just by changing the position of

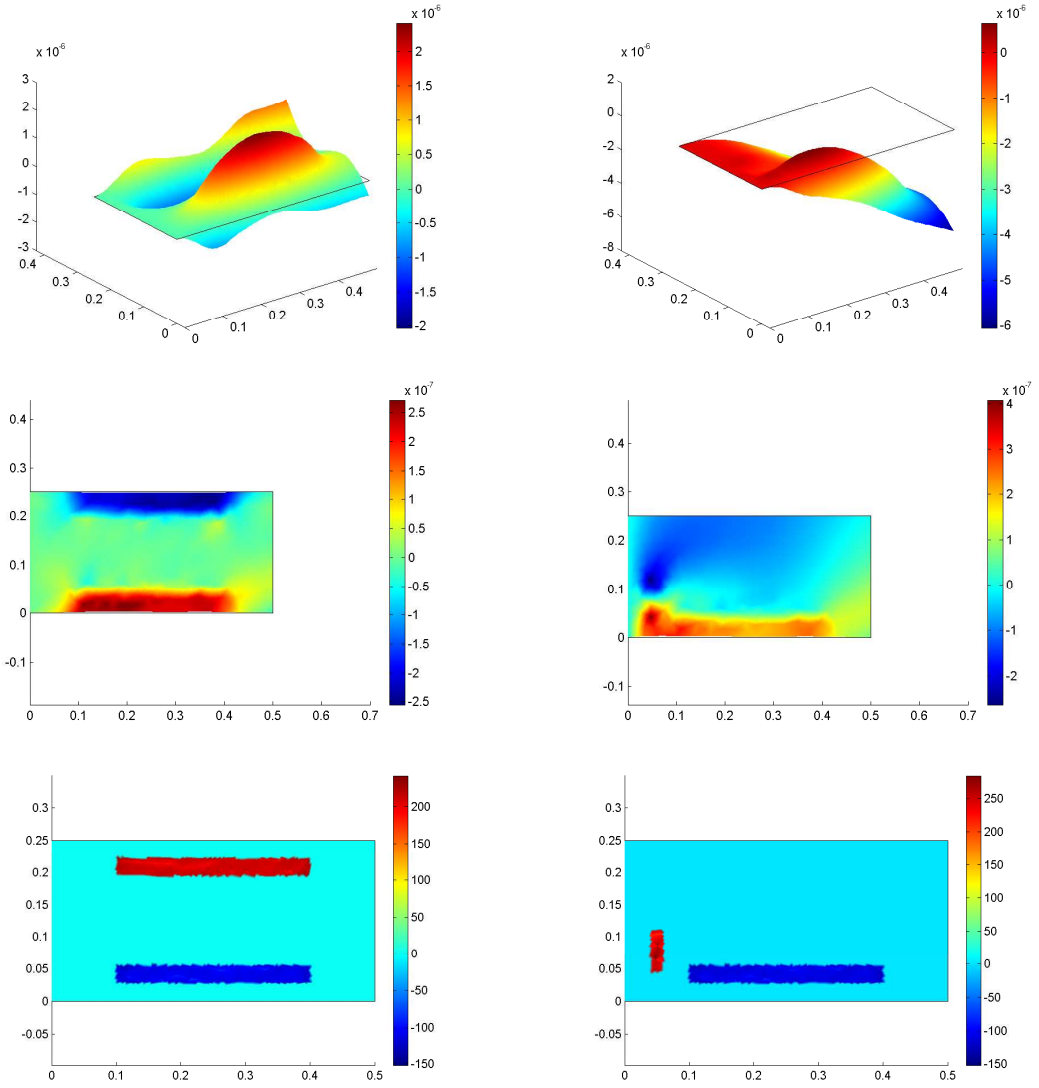

FIGURE 4. Two elastic plates with two bonded surface piezoelectric patches (PSBP), subject to the same data, except the position of the upper patches: in the left column $\omega^+ = [0.5, 4 * 0.5/5] \times [7 * 0.25/9, 8 * 0.25/9]$ and in the right column $\omega^+ = [0.04, 0.06] \times [0.045, 2 * 0.055]$. Top row: differences for the transverse displacement ξ_3. Middle row: differences for the deformed middle plane of the plate (multiplied by 10^4) in the tangential directions. Bottom row: the distinct positions of ω^+ and the different values of the electric potentials φ^+ and φ^-.

the upper patch, and keeping the other data equal for the two plates. More precisely, both plates are subject to electric boundary conditions $(ebc1^{mat})$,

for both materials $mat = +, -$, with $\varphi^{+}_{0lo} - \varphi^{+}_{0up} = \varphi^{-}_{0lo} - \varphi^{-}_{0up} = 100$, $\varphi^{+}_{0lo} = 100$, $\varphi^{-}_{0lo} = 100$, and for the lower patch $\omega^{-} = [0.5, 4 * 0.5/5] \times [0.25/9, 2 * 0.25/9]$. But the positions of the upper patches are different: for one plate $\omega^{+} = [0.5, 4 * 0.5/5] \times [7 * 0.25/9, 8 * 0.25/9]$ (left column) and for the other plate $\omega^{+} = [0.04, 0.06] \times [0.045, 2 * 0.055]$ (the right column). The first row demonstrates the differences for the transverse displacements of the middle plane of the plate. The second row exhibits the differences for the deformed middle plane of the plate (multiplied by 10^4) in the tangential directions. The last row contains the visual representation of the patches' positions as well as the values of the electric potentials φ^{+} and φ^{-}, for the two cases.

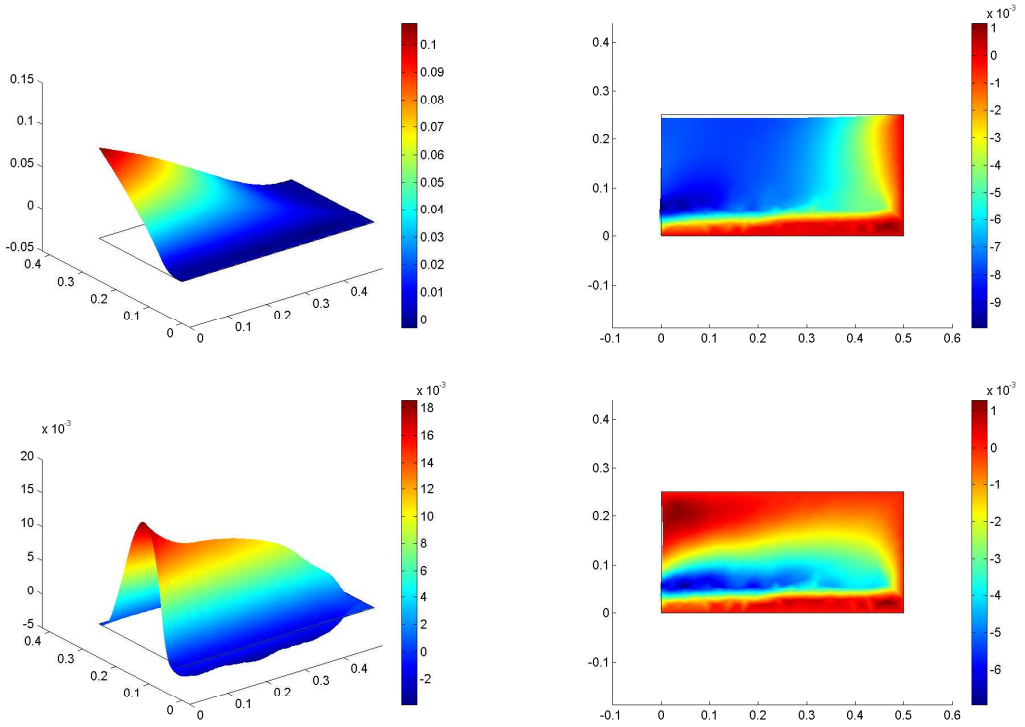

FIGURE 5. Elastic plate with two bonded surface piezoelectric patches (PSBP), verifying the conditions of corollary 3.2. Left column: transverse displacements ξ_3 (the plate verifies assumptions i) of corollary 3.2). Right column: deformed middle plane of the plate in the tangential directions (the plate verifies assumptions ii) of corollary 3.2). The plate is clamped in two consecutive sides (top row), and in three sides (bottom row).

In Figure 5 we have once more a plate of type PSBP, but now we assume it verifies the assumptions of corollary 3.2. Hence the electric boundary

conditions are $(ebc2^{mat})$ for both patches and $\omega^+ = \omega^- = [0, 0.5] \times [0.25/9, 2 * 0.25/9]$. Figure 5 shows the graphics of the transverse displacements ξ_3, when the density of the surface electric charges of the patches verify $\theta^+ = -\theta^- = 10$ (left column), and the graphics of deformed middle plane of the plate in the tangential directions, when $\theta^+ = \theta^- = 10$ (right column). Moreover in the top row the plate is clamped in two consecutive sides and for the bottom row it is clamped in three sides.

In Figure 6 we have again a plate of type PSBP, whose patches verify the electric boundary conditions $(ebc2^{mat})$, for $mat = +, -$. But in this example, $\omega^+ \neq \omega^-$, more precisely, $\omega^+ = [0.5, 4 * 0.5/5] \times [7 * 0.25/9, 8 * 0.25/9]$ and $\omega^- = [0.5, 4 * 0.5/5] \times [0.25/9, 2 * 0.25/9]$. Thus the plate does not verify the assumptions of corollary 3.2. This Figure 6 presents the differences observed in the mechanical displacements and electric potentials, when we just modify the densities of the surface electric charges of the patches. In the left column $\theta^+ = \theta^- = 10$ and in the right column $\theta^+ = 10$, $\theta^- = -1$. Moreover the plate is clamped in only one side.

In Figure 7 we study the case of two plates of type PIP, which only differ on the location of the inserted patch. The electric boundary conditions are $(ebc1^p)$ with $\varphi_{0up} = 0$, $\varphi_{0lo} = 10$, and the only no-zero mechanical data is $f_3 = 1$ which acts in the elastic part. This Figure 7 displays the differences for the transverse mechanical displacement ξ_3, the deformed middle plane of the plate in the tangential directions, and the electric potential for the two cases: when $\omega^p = [0.1, 0.4] \times [0.25/9, 2 * 0.25]$ (left column), and when $\omega^p = [0.04, 0.1] \times [0.045, 0.15]$ (right column). In addition it is supposed that these plates are clamped in two opposite sides.

In Figure 8 reports the differences in the mechanical displacements and electric potentials, for two plates of type PIP, which are subject to electric boundary conditions $(ebc2^p)$ and have just the same mechanical, electric and geometrical data, apart from the value of the surface electric charge densities: for one plate $\theta = 0$ (left column) and for the other plate $\theta = 10$ (right column). Big differences appear in the deformed middle plane of the plate and the values of the electric potential φ. The components of the mechanical forces, acting only in the elastic part, are $f_1 = -10$, $f_2 = 10$, $f_3 = 10$, for both plates, and they are also clamped in three lateral sides.

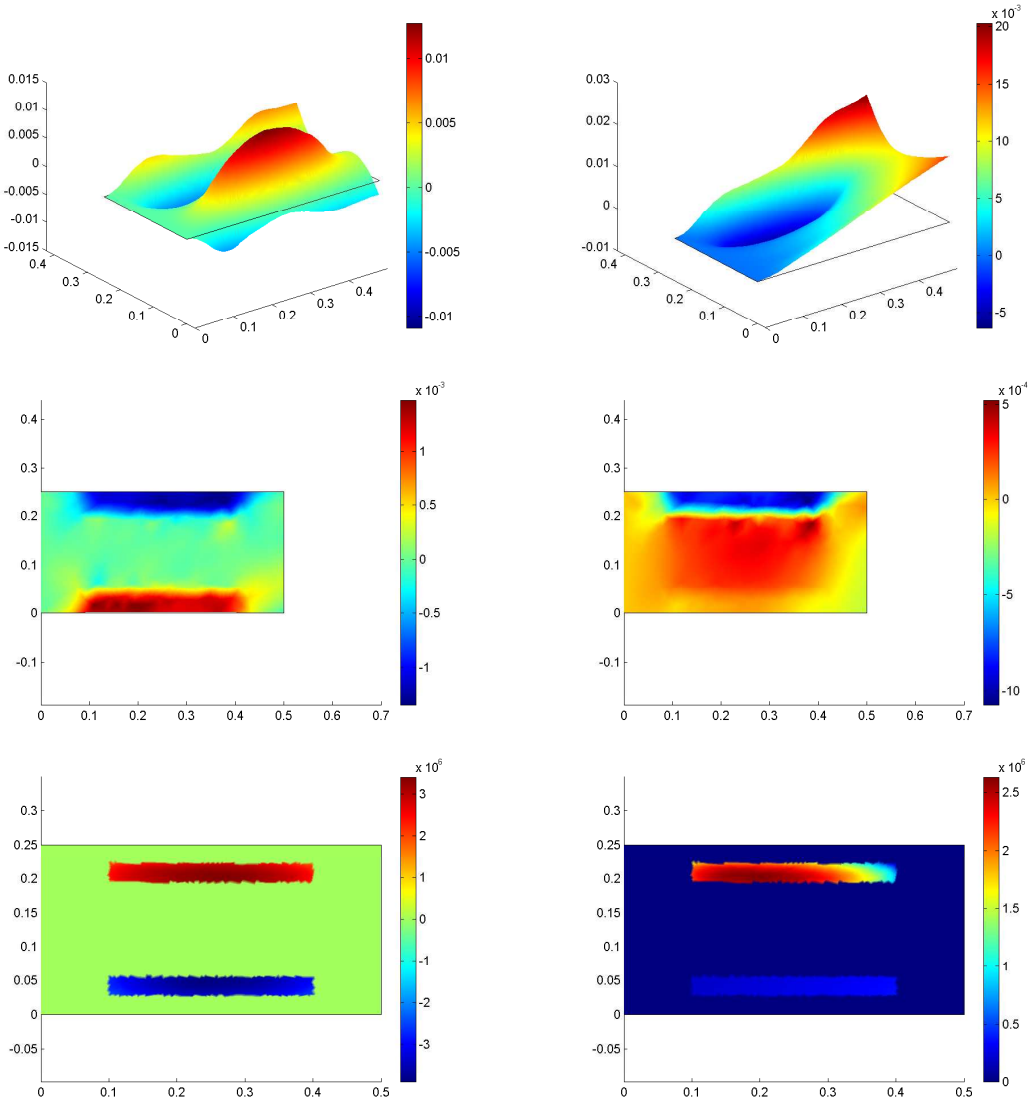

FIGURE 6. Elastic plate with two no-symmetric bonded surface piezoelectric patches (PSBP) and different surface electric charges densities: $\theta^+ = \theta^- = 10$ (left) and $\theta^+ = 10$, $\theta^- = -1$ (right). Transverse displacements ξ_3 (top row), deformed middle plane of the plate in the tangential directions (middle row), and electric potentials (bottom row).

References

[1] M. Barboteu, J. R. Fernández, and Y. Ouafik. Numerical analysis of two frictionless elastic-piezoelectric contact problems. *J. Math. Anal. Appl.*, 339(2):905–917, 2008.

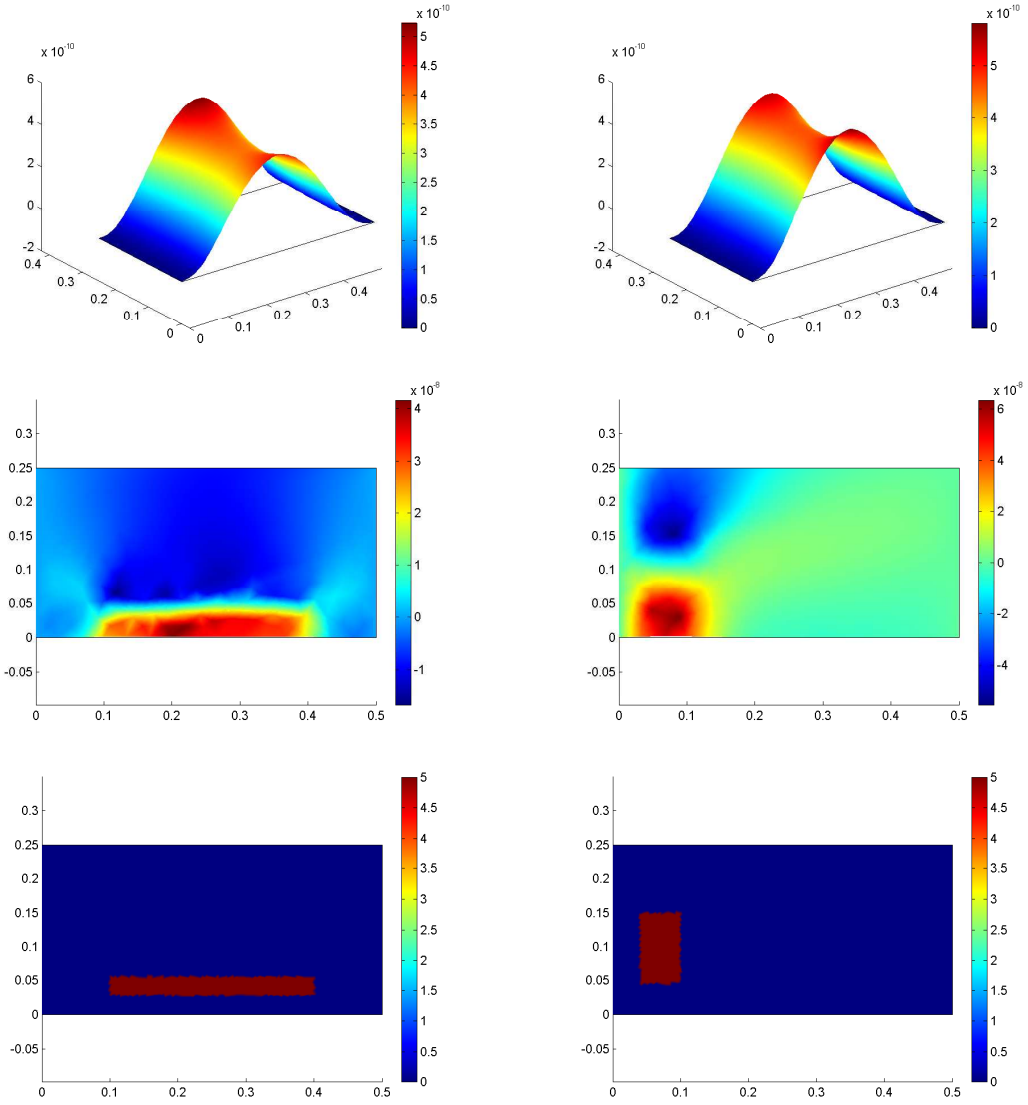

FIGURE 7. Two elastic plates with inserted piezoelectric patches (PIP) in different positions: $\omega^p = [0.1, 0.4] \times [0.25/9, 2 * 0.25]$ (left), and $\omega^p = [0.04, 0.1] \times [0.045, 0.15]$ (right). Top row: transverse displacements ξ_3. Second row: deformed middle plane of the plate in the tangential directions. Fourth row: electric potential and position of the patches.

[2] M. Barboteu, J. R. Fernández, and Y. Ouafik. Numerical analysis of a frictionless viscoelastic piezoelectric contact problem. *ESAIM: Mathematical Modelling and Numerical Analysis (M2AN)*, to appear 2008.

[3] M. Barboteu, J. R. Fernández, and T. Raffat. Numerical analysis of a dynamic piezoelectric contact problem arising in viscoelasticity. *Computer Methods in Applied Mechanics and Engineering*, to appear 2008.

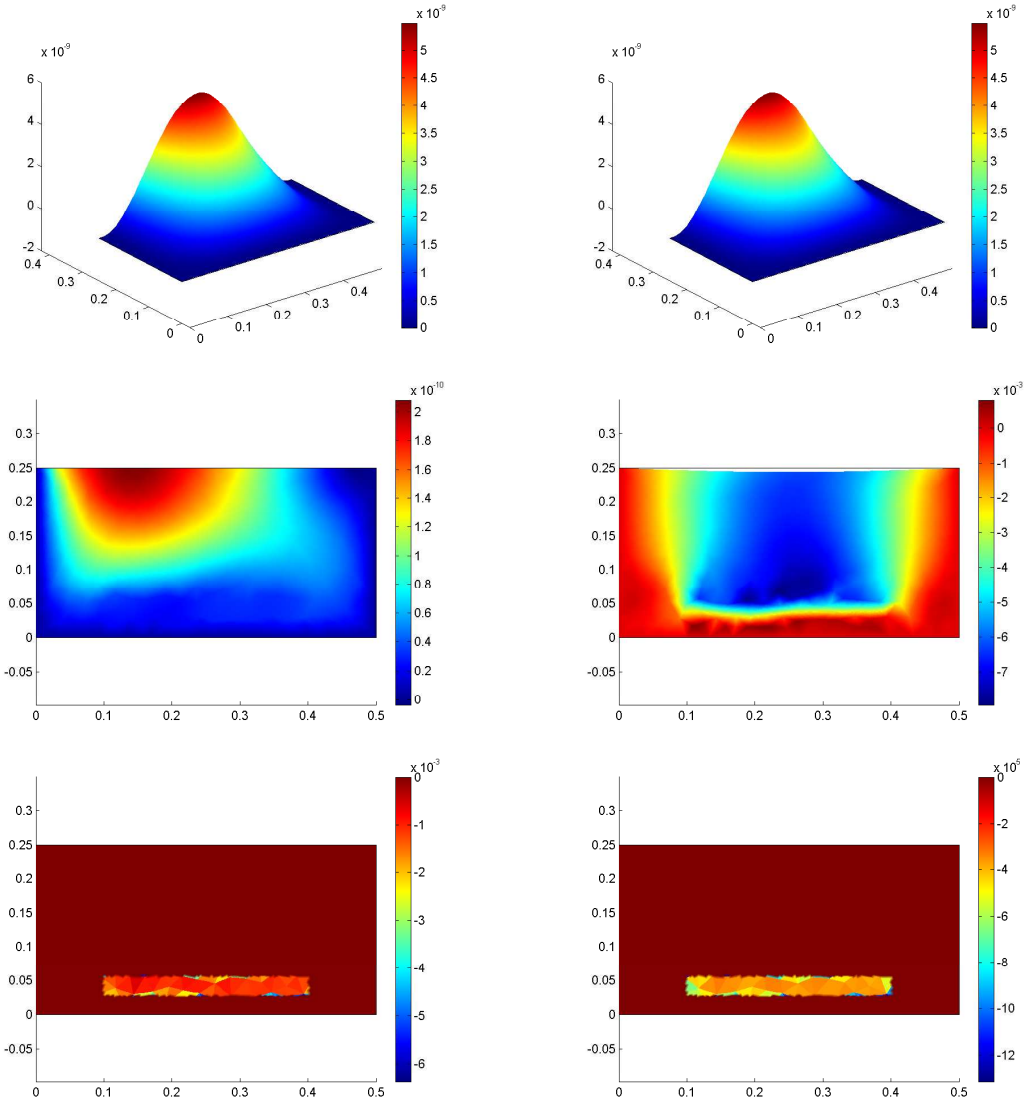

FIGURE 8. Two elastic plates with inserted piezoelectric patches (PIP) sharing the same mechanical, electric and geometric data, except the value of θ: $\theta = 0$ (left) and $\theta = 10$ (right). Top row: transverse displacements ξ_3. Second row: deformed middle plane of the plate in the tangential directions. Fourth row: electric potential and position of the patches.

[4] M. Bernadou and C. Haenel. Modelization and numerical approximation of piezoelectric thin shells. III. From the patches to the active structures. *Comput. Methods Appl. Mech. Engrg.*, 192(37-38):4075–4107, 2003.

[5] P. G. Ciarlet and P. Destuynder. Une justification d'un modèle non linéaire en théorie des plaques. *C. R. Acad. Sci. Paris Sér. A-B*, 287(1):A33–A36, 1978.

[6] P. G. Ciarlet and P. Destuynder. A justification of the two-dimensional linear plate model. *J. Mécanique*, 18(2):315–344, 1979.
[7] P. G. Ciarlet. *Plates and junctions in elastic multi-structures*, volume 14 of *Recherches en Mathématiques Appliquées [Research in Applied Mathematics]*. Masson, Paris, 1990. An asymptotic analysis.
[8] P. G. Ciarlet. *Mathematical elasticity. Vol. II*, volume 27 of *Studies in Mathematics and its Applications*. North-Holland Publishing Co., Amsterdam, 1997. Theory of plates.
[9] P. G. Ciarlet. *Mathematical elasticity. Vol. III*, volume 29 of *Studies in Mathematics and its Applications*. North-Holland Publishing Co., Amsterdam, 2000. Theory of shells.
[10] Ch. Collard and B. Miara. Two-dimensional models for geometrically nonlinear thin piezoelectric shells. *Asymptot. Anal.*, 31(2):113–151, 2002.
[11] Comsol Multiphysics®. *http://www.comsol.com/*.
[12] L. Costa, I. Figueiredo, R. Leal, P. Oliveira, and G. Stadler. Modeling and numerical study of actuator and sensor effects for a laminated piezoelectric plate. *Comput. Struct.*, 85:385–403, 2007.
[13] J. R. Fernández and K. L. Kuttler. An existence and uniqueness result for an elasto-piezoelectric problem with damage. *Mathematical Models and Methods in the Applied Sciences*, to appear 2008.
[14] J. R. Fernández, R. Martínez, and G. E. Stavroulakis. Numerical analysis of an elasto-piezoelectric problem with damage. *International Journal for Numerical Methods in Engineering*, to appear 2008.
[15] I. Figueiredo and C. Leal. A piezoelectric anisotropic plate model. *Asymptot. Anal.*, 44(3-4):327–346, 2005.
[16] I. Figueiredo and C. Leal. A generalized piezoelectric Bernoulli-Navier anisotropic rod model. *J. Elasticity*, 85(2):85–106, 2006.
[17] I. Figueiredo and G. Stadler. Frictional contact of an anisotropic piezoelectric plate. *ESAIM: Control, Optimisation and Calculus of Variations (COCV)*, to appear 2008.
[18] S. Hüeber, A. Matei, and B. I. Wohlmuth. A mixed variational formulation and an optimal a priori error estimate for a frictional contact problem in elasto-piezoelectricity. *Bull. Math. Soc. Sci. Math. Roumanie (N.S.)*, 48(96)(2):209–232, 2005.
[19] S. Klinkel and W. Wagner. A geometrically non-linear piezoelectric solid shell element based on a mixed multi-field variational formulation. *Int. J. Numer. Meth. Engng*, 65(3):349–382, 2005.
[20] G. A. Maugin and D. Attou. An asymptotic theory of thin piezoelectric plates. *Quart. J. Mech. Appl. Math.*, 43(3):347–362, 1990.
[21] M. Rahmoune, A. Benjeddou, and R. Ohayon. New thin piezoelectric plate models. *J. Int. Mat. Sys. Struct.*, 9:1017–1029, 1998.
[22] M. Rahmoune. *Plaques intelligentes piézoélectriques: Modélisation et applications au contrôle santé*. PhD Thesis, Univerité Paris VI, 1997.
[23] A. Raoult and A. Sène. Modelling of piezoelectric plates including magnetic effects. *Asymptot. Anal.*, 34(1):1–40, 2003.
[24] N. Sabu. Vibrations of thin piezoelectric flexural shells: two-dimensional approximation. *J. Elasticity*, 68(1-3):145–165 (2003), 2002.
[25] A. Sene. Modelling of piezoelectric static thin plates. *Asymptot. Anal.*, 25(1):1–20, 2001.
[26] R. Smith. *Smart material systems*, volume 32 of *Frontiers in Applied Mathematics*. Society for Industrial and Applied Mathematics (SIAM), Philadelphia, PA, 2005. Model development.
[27] M. Sofonea and El-H. Essoufi. A piezoelectric contact problem with slip dependent coefficient of friction. *Math. Model. Anal.*, 9(3):229–242, 2004.

[28] M. Sofonea and El-H. Essoufi. Quasistatic frictional contact of a viscoelastic piezoelectric body. *Adv. Math. Sci. Appl.*, 14(2):613–631, 2004.
[29] L. Trabucho and J. M. Viaño. Mathematical modelling of rods. In *Handbook of numerical analysis, Vol. IV*, Handb. Numer. Anal., IV, pages 487–974. North-Holland, Amsterdam, 1996.
[30] T. Weller and C. Licht. Analyse asymptotique de plaques minces linéairement piézoélectriques. *C. R. Math. Acad. Sci. Paris*, 335(3):309–314, 2002.

José A. Carvalho
Department of Mathematics, University of Coimbra, Apartado 3008, 3001-454 Coimbra, Portugal, and Escola Superior de Tecnologia de Setúbal, Portugal.
E-mail address: jcarvalho@est.ips.pt

Isabel N. Figueiredo
Centro de Matemática da Universidade de Coimbra (CMUC), Department of Mathematics, University of Coimbra, Apartado 3008, 3001-454 Coimbra, Portugal.
E-mail address: isabelf@mat.uc.pt

Rebeca Martínez
Departamento de Matemática Aplicada, Universidade de Santiago de Compostela, Facultade de Matemáticas, Campus Sur s/n, 15782 Santiago de Compostela, Spain.
E-mail address: rebeca.martinez2@rai.usc.es